Prethermalization and thermalization of a quenched interacting Luttinger liquid

Michael Buchhold, Markus Heyl, Sebastian Diehl

Angaben zur Veröffentlichung / Publication details:

Buchhold, Michael, Markus Heyl, and Sebastian Diehl. 2016. "Prethermalization and thermalization of a quenched interacting Luttinger liquid." *Physical Review A* 94 (1): 013601. https://doi.org/10.1103/physreva.94.013601.

Prethermalization and thermalization of a quenched interacting Luttinger liquid

Michael Buchhold,[1] Markus Heyl,[2] and Sebastian Diehl[1]
[1]*Institut für Theoretische Physik, Universität zu Köln, D-50937 Cologne, Germany*
[2]*Physik Department, Technische Universität München, 85747 Garching, Germany*
(Received 23 May 2016; published 8 July 2016)

We study the relaxation dynamics of interacting one-dimensional fermions with band curvature after a weak quench in the interaction parameter at zero temperature. Our model lies within the class of interacting Luttinger liquids, where the harmonic Luttinger theory is extended by a weak-integrability-breaking phonon scattering term. In order to solve for the nonequilibrium time evolution, we use quantum kinetic equations exploiting the resonant but subleading character of the phonon interaction term. The interplay between phonon scattering and the quadratic Luttinger theory leads to the emergence of three distinct spatiotemporal regimes for the fermionic real-space correlation function. It features the crossover from a prequench to a prethermal state, finally evolving towards a thermal state on increasing length and time scales. The characteristic algebraically decaying real-space correlations in the prethermalized regime become modulated by an amplitude that is decaying in time according to a stretched exponential as an effect of the interactions. The asymptotic thermalization dynamics is governed by energy transport over large distances from the thermalized to the nonthermalized regions via macroscopic, dynamical slow modes. This is revealed in an algebraic decay of the system's effective temperature. The numerical value of the associated exponent agrees with the dynamical critical exponent of the Kardar-Parisi-Zhang universality class. We also discuss a criterion for the applicability of this theory away from the integrable limit of noninteracting fermions.

DOI: 10.1103/PhysRevA.94.013601

I. INTRODUCTION

It is a property of fundamental importance within statistical physics that generic and realistic thermodynamic systems exhibit one particular state, thermal equilibrium, which is always approached, irrespective of the initial condition. Yet the important question of which microscopic conditions are necessary or sufficient for the thermalization of a closed quantum many-body system is still largely unanswered [1]. This is of particular importance, especially because there exists a specific class of isolated quantum systems, termed integrable, for which relaxation to thermal states is prevented due to the presence of an extensive number of (quasi)local conservation laws [2–4]. Such particular systems often represent isolated points in the parameter space of physical many-body systems and demand a precise tuning of the microscopic parameters. Nevertheless, these models are very valuable because they often represent fixed points of renormalization-group theories and as such contain the low-temperature equilibrium properties of a much wider class of systems. This directly leads to an apparent dilemma in quantum many-body theory that has attracted a great deal of interest recently. In particular, beyond equilibrium these integrable models become nongeneric as they fail to thermalize. Instead, they are trapped in extended prethermal states described by nonthermal generalized Gibbs ensembles [1–8]. Resolving this dilemma is one of the major challenges for the understanding of the coherent dynamics of quantum many-body systems.

In this work we address this question for a paradigmatic low-energy model: the Luttinger liquid [9–11], representing the fixed point theory of systems of interacting fermionic particles in one dimension at low temperatures. The Luttinger liquid is an integrable theory failing to thermalize but rather exhibiting a description in terms of a generalized Gibbs ensemble [6,12,13]. Here we will be interested in the nonequilibrium dynamics in the presence of a weak fermionic band curvature, which represents a generic perturbation, irrelevant in the low-energy equilibrium limit, but relevant on intermediate to long-time scales in order to drive the crossover towards thermalization.

The increasing number of cold-atom experiments performed under out-of-equilibrium conditions [14–23] has driven significant interest in the theoretical understanding of the nonequilibrium dynamics in quantum many-body systems. Importantly, these experiments share a remarkable isolation from the environment, thereby probing the purely coherent unitary time evolution on the experimentally relevant time scales. This has paved the way to experimentally study the constrained relaxational dynamics of quantum systems close to integrability [15,24–26], showing unconventional properties due to the anticipated (quasi)local conservation laws. Although the inherent integrability-breaking terms, resulting from, e.g., imperfections in the particle-particle interactions or higher orbital modes, are considered to be weak, they are believed to eventually cause relaxation to thermal states on long-time scales. Yet a full understanding of this process has not been achieved so far. Within the current understanding, however, the thermalization dynamics of quantum many-body systems with weak-integrability-breaking perturbations is expected to occur via a two-stage process. Initially, the dynamics of local observables at transient and intermediate-time scales are controlled by the corresponding integrable theory serving as a metastable attractor for the nonintegrable dynamics [4,27,28]. This trapping in a metastable state has been termed prethermalization [27,29] and is expected to exist for several nonintegrable models and models close to integrability [4,27,30–38]. In the quasiparticle picture, prethermalization is associated with the initial formation of well-defined excitations [27], which leads to a dephasing of all terms that are not diagonal in quasiparticle modes, i.e., to a projection of the initial density

matrix onto the diagonal ensemble in the quasiparticle basis. After this intermediate quasiparticle formation, the dynamics eventually crosses over to the thermalization regime, where weak quasiparticle scattering leads to a slow redistribution of energy and establishes detailed balance between the different modes. This causes asymptotic thermalization on long-time scales compatible with the eigenstate thermalization hypothesis [5,39–42].

In equilibrium, the fermionic band curvature in the Luttinger liquid, because irrelevant in the renormalization-group sense, does not modify static correlation functions, which are well described by the quadratic Luttinger theory. Importantly, however, the curvature has a strong impact on frequency-resolved fermionic quantities. This has been observed in Coulomb drag experiments [43,44], which could not be explained in terms of a quadratic Luttinger theory. In a hydrodynamic representation, the band curvature describes resonant scattering processes between the elementary phononic excitations of the system such that perturbation theory is plagued by divergences due to the resonant nature of the interactions. Important early approaches to the interacting Luttinger liquid applied a self-consistent Born approximation in order to determine the phonon self-energy on the mass shell [45–47]. However, these works were unable to explain the frequency dependence of the self-energy, which appeared to be non-negligible for dynamic observables. Using a combination of bosonization and subsequent refermionization, a general theory has been developed that has been very successful in determining spectral equilibrium properties such as the dynamic structure factor and the fermionic spectral function in thermal equilibrium [48–51]. Importantly for the scope of the present work, however, it has not yet been possible to generalize this methodology to systems out of equilibrium. Only recently, these equilibrium results have been recovered by a quantum hydrodynamic approach [52,53], showing that hydrodynamics is also capable of controlling the resonant phonon interactions.

The theoretical finding of these works is that the elementary excitations are no longer described in terms of bosonic quasiparticles with an exact energy-momentum relation $\omega = u|q|$ but dissolve into a continuum of excitations. This continuum, however, is energetically confined between two well-defined excitation branches $\epsilon_q^- < \omega < \epsilon_q^+$ (with $\epsilon_q^\pm \to 0$ as $q \to 0$) at which the spectral weight of the bosonic excitations features algebraic divergences, reflected in corresponding divergences of the dynamical structure factor. This fine structure in the bosonic spectral weight, and equivalently self-energy, makes the development of a general kinetic theory for *frequency-resolved* observables a very demanding task, which has not yet found a satisfactory solution. However, as will be shown in this work, static properties and their time evolution are nevertheless accessible.

The goal of this work is to study the escape out of the prethermalization regime and the crossover towards thermalization in Luttinger liquids with quadratic fermionic dispersion on the basis of a hydrodynamic description. Specifically, we aim at formulating a kinetic theory for the momentum distribution of the phononic degrees of freedom taking into account the leading nonlinear corrections due to the quadratic dispersion. While in this way we are able to describe the escape out of the prethermalization regime in a controlled way, the final asymptotic thermalization of the system might be modified by the more subleading off-resonance contributions, which we do not consider here. The kinetic equation describes the time evolution of the phonon momentum distribution and is suitable in the long-wavelength limit and for weak quenches but still goes beyond the regime of linear response. In turn this kinetic theory gives a valid description for the fermionic occupation distribution in the vicinity of the Fermi points where the anticipated fine structure of the bosonic spectral weight only gives subleading contributions. This semistatic, and as a consequence tractable, description covers the forward-time evolution of any static, i.e., frequency-independent, observable. We show that the dynamics of precisely these frequency-independent observables depend only on the time evolution of the momentum distribution of excitations n_q and can be captured within a kinetic theory. The justification for this approach is the subleading width of the excitation spectrum $|\epsilon_q^+ - \epsilon_q^-| \ll u|q|$ compared to the phonon energy for all relevant q (below the Luttinger liquid cutoff), which is equivalent to the statement that even in the presence of the nonlinearity the continuum of excitations in the hydrodynamic description is tightly bound to the mass shell. This condition replaces the common quasiparticle criterion [54] and enables a thorough kinetic description.

The applicability of the kinetic equation requires the preformation of well-defined quasiparticles out of the bare particles, which occurs during the process of prethermalization before the quasiparticle scattering sets in. We find, however, that close to the integrable point of vanishing fermionic interactions, quasiparticle formation becomes very slow, shifting the applicability of the theory for weakly interacting fermions to long-time scales and far distances. We give quantitative estimates of the corresponding spatiotemporal scales of the breakdown of the kinetic theory. Not too close to the noninteracting point, however, the kinetic equation is well justified and allows us to study the escape out of the prethermalization regime towards thermalization. In the regime of applicability, the kinetic equation leads in the asymptotic long-time limit to a linearized quantum Boltzmann equation whose attractor is the desired thermal Gibbs state. We find that the thermalization dynamics out of the prethermal state is triggered by short-wavelength modes and afterward progresses algebraically slowly towards longer wavelengths. Whether this is a generic feature of weakly perturbed integrable theories is an important and interesting question for future work.

The main result of this work is a spatiotemporal decomposition of correlations in the studied nonlinear Luttinger liquid, which is illustrated in Fig. 1. By analyzing the equal-time fermionic Green's function $G^<_{\mathrm{t},x}$, the Fourier transform of the fermionic occupation distribution, we find three regimes, which we term prequench, prethermal, and thermal, that are separated by two crossover scales $x_{\mathrm{th}}(t)$ and $x_{\mathrm{pt}}(t)$ obeying $x_{\mathrm{th}}(t) < x_{\mathrm{pt}}(t)$. The crossover scale $x_{\mathrm{pt}}(t) = 2ut$ sets the light cone [7] with u the sound velocity of the elementary bosonic excitations of the integrable theory. Causality implies that for distances $x \gg x_{\mathrm{pt}}(t)$ the system's properties are not yet influenced by the nonequilibrium protocol, but are rather given by the initial state yielding the notion of the prequench regime. Inside the light cone for distances $x < x_{\mathrm{pt}}(t)$ we identify a

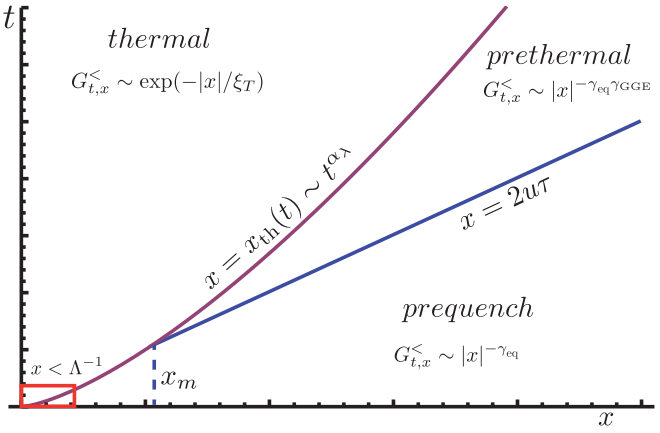

FIG. 1. Illustration of the spatiotemporal thermalization and prethermalization dynamics in terms of the fermionic Green's function $G^<_{t,x}$. For long distances $x > 2ut$ and $x > x_{\rm th}$, the Green's function is determined by the quasiparticles of the initial state and feature algebraic decay in real space corresponding to the prequench state of the system, modulated by a amplitude decaying as a stretched exponential in time. In the intermediate regime $2ut < x < x_{\rm th}(t)$, the corresponding quasiparticles correspond to the postquench Hamiltonian but are distributed according to a nonequilibrium distribution function, inducing a prethermal real-space scaling behavior $|G^<_{t,x}| \sim |x|^{-\gamma_{\rm eq}\gamma_{\rm GGE}}$. For short distances $x < x_{\rm th}(t)$, the Green's function is thermal, $\sim \exp -|x|/\xi_T$, described by an effective temperature $\tilde{T}_t$ and a corresponding thermal correlation length ξ_T. The scaling $x_{\rm th}(t) \sim t^{\alpha_\lambda}$, $\alpha < 1$, implies that there exists a minimal distance x_m for which no clear prethermal regime can be identified since the scattering of quasiparticles is equally faster than the formation of quasiparticles. In this regime, the kinetic theory cannot be applied. The short-distance regime $x < \Lambda^{-1}$, for which Luttinger theory is invalid, occupies a negligibly small short-time regime.

further crossover scale $x_{\rm th}(t)$ separating the prethermal and thermal spatial regions. For distances $x_{\rm th}(t) \ll x \ll x_{\rm pt}(t)$ the system's spatial correlations are controlled by the integrable theory, which for long times are determined by the associated generalized Gibbs ensemble. This regime is therefore called prethermal. Interestingly, the thermalization dynamics, triggered by the weak fermionic nonlinearity, sets in at even smaller scales $x \ll x_{\rm th}(t)$. At these distances, the correlations approach their thermal form. However, the associated effective temperature $\tilde{T}_t$ is larger than the expected temperature T for the asymptotic fully thermalized state. Instead $\tilde{T}_t$ is a dynamical quantity approaching T only algebraically slowly due to macroscopic dynamical slow modes.

Kinetic equations have been successfully applied to Luttinger liquids with a cosine potential, resulting from particle backscattering in Refs. [55,56]. For Luttinger liquids with cubic interactions a kinetic equation approach has been derived in Ref. [57]. The latter makes use of nonperturbative Dyson-Schwinger equations in order to solve the time evolution of the phonon distribution function in the presence of the renormalization-group-irrelevant but resonant interactions. This kinetic equation approach is particularly well suited for Luttinger models close to the ground state, i.e., with a small number of phononic excitations, but can also be applied to excited states as long as the Luttinger criterion is satisfied locally, i.e., as long as the phonon density $n_q < \Lambda/|q|$ for all momenta $|q|$. Based on Ref. [57], we can give explicit criteria for the validity of this approach for the fermionic dynamics after we have introduced the quench scenario.

This paper is organized as follows. We introduce the studied model system, the interacting Luttinger liquid, in Sec. II. The main results are summarized in Sec. III. The derivation of the kinetic equations, which is used to solve the complex quantum many-body problem, is presented in Sec. V. It is analyzed and numerically solved in Sec. VI, where we also give the derivation of the main results.

II. INTERACTING LUTTINGER LIQUID

The simplest form of an interacting Luttinger liquid emerges as the effective long-wavelength description of spinless interacting fermions with quadratic (i.e., dispersive) corrections to a perfectly linear dispersion around the Fermi energy [9,10,58,59]. Although the fermionic band curvature is irrelevant in the sense of the renormalization group (RG) [58] and therefore does not modify the static infrared behavior of the fermions, it is visible in dynamic observables, such as the fermionic spectral function or the dynamical structure factor [47,60–64]. In this work we will show that in a nonequilibrium situation, the quasiparticle scattering induced by the band curvature leads to a dynamical redistribution of energy and allows the system to relax towards a thermal state. Thus, the system becomes generic. This kind of relaxation is absent for nondispersive fermions, since the corresponding model, the linear Luttinger model, is integrable. The fermionic band curvature breaks the integrability of the linear model and therefore, even though RG irrelevant, is the leading-order term that drives the system away from a prethermal, i.e., generalized Gibbs ensemble (GGE) -type, dynamical fixed point and towards a thermal one.

The Luttinger liquid in its fermionic representation is described in terms of left- and right-moving spinless fermions (labeled with $\eta = \pm$), created and annihilated by operators $\psi^\dagger_{\eta,x}, \psi_{\eta,x}$. The Hamiltonian is

$$H = -\sum_\eta \int_x \psi^\dagger_{\eta,x}\left(i\eta v_{\rm F}\partial_x + \frac{1}{2m}\partial_x^2\right)\psi_{\eta,x} + \frac{1}{2}\int_{x,x'} g(x-x')\rho_x\rho_{x'}, \tag{2.1}$$

with the combined density $\rho_x = \rho_{+,x} + \rho_{-,x} = \psi^\dagger_{+,x}\psi_{+,x} + \psi^\dagger_{-,x}\psi_{-,x}$. The interaction, characterized by $g(x-x')$, is supposed to be short ranged in space (decaying faster than algebraic) but has a short-distance cutoff of the order of the Luttinger cutoff Λ^{-1}. In the long-wavelength limit, particles with a wavelength larger than the effective range of the potential only experience a contact potential $g(q) = g_0$, where g_0 is the interaction strength at zero momentum. In order to regularize the interaction in the ultraviolet (UV) regime, which is required to obtain a nondiverging quench-induced interaction energy, it is cut off at the UV scale Λ, i.e., $g(q) = g_0\theta(\Lambda - |q|)$.

The bosonized version of the Hamiltonian in the absence of band curvature describes the well-known Luttinger model

$$H_{\mathrm{LL}} = \int_x u K (\partial_x \theta_x)^2 + \frac{u}{K} (\partial_x \phi_x)^2 \tag{2.2}$$

with sound velocity $u = \frac{v_{\mathrm{F}}}{K}$ and Luttinger parameter $K = (1 + \frac{g_0}{\pi v_{\mathrm{F}}})^{-1/2}$. In addition, due to the fermionic band curvature, a cubic nonlinearity occurs [47,52,60,61,65]

$$H_{\mathrm{NL}} = \frac{1}{m} \int_x (\partial_x \theta_x)^2 \partial_x \phi_x \tag{2.3}$$

such that the complete bosonized Hamiltonian is $H = H_{\mathrm{LL}} + H_{\mathrm{NL}}$. Due to the linear dispersion of the Luttinger quasiparticles, H_{NL} describes scattering processes on a highly degenerate bosonic manifold, i.e., is governed by a large set of energy-conserving scattering processes. This leads to diverging perturbative corrections at any order of perturbation theory. The bosonized fermionic interaction is quadratic in the Luttinger fields, while the band curvature transforms into a cubic nonlinearity proportional to $\frac{1}{m}$.

In the following, we will consider a nonequilibrium scenario in terms of an interaction quench. Initially, the system is supposed to be prepared in the ground state of the integrable Luttinger liquid theory at an interaction potential $g^i(x)$. Due to the interaction quench, the interaction potential is suddenly switched at time $t = 0$ from an initial to a final value

$$g(x) = \begin{cases} g^i(x) & \text{for } t < 0 \\ g^f(x) & \text{for } t > 0 \end{cases} \tag{2.4}$$

and both the quadratic Hamiltonian and the nonlinearity are modified by this interaction change. The eigenbasis of H_{LL}, which is expressed in terms of the physically more transparent phononic creation and annihilation operators $a_q^\dagger, a_q$ according to the canonical Bogoliubov transformation

$$\theta_x = \theta_0 + \frac{i}{2} \int_q \left(\frac{2\pi}{|q| K} \right)^{1/2} e^{-iqx - |q|/\Lambda} (a_q^\dagger - a_{-q}), \tag{2.5}$$

$$\phi_x = \phi_0 - \frac{i}{2} \int_q \left(\frac{2\pi K}{|q|} \right)^{1/2} \mathrm{sgn}(q) e^{-iqx - |q|/\Lambda} (a_q^\dagger + a_{-q}), \tag{2.6}$$

is therefore obviously transformed by the quench. This transformation depends on the interaction via the Luttinger parameter K.

The state of the system before the quench no longer corresponds, in general, to an equilibrium state after the quench and the system will consequently undergo a nontrivial time evolution according to the new Hamiltonian. The occupations of bosonic modes after the quench can be computed via the above Bogoliubov transformation. Before the quench, the interacting system is in equilibrium at zero temperature such that $G^K_{q,t=0} = \langle \{a_q, a_q^\dagger\} \rangle = 1$ in the prequench basis. This yields the postquench occupations

$$n_{t=0,q} = \langle a_q^\dagger a_q \rangle_{t=0} = \frac{1}{2} \left[\frac{\lambda^2 + 1}{\lambda} n_{i,q} + \frac{(\lambda - 1)^2}{2\lambda} \right],$$

$$m_{t=0,q} = \langle a_q^\dagger a_{-q}^\dagger \rangle_{t=0} = \frac{1 - \lambda^2}{4\lambda} (2 n_{i,q} + 1), \tag{2.7}$$

with $\lambda = \frac{K_{\mathrm{f}}}{K_{\mathrm{i}}}$. Here $n_{i,q}$ is the initial occupation of the bosonic modes and $\lambda = \frac{K_{\mathrm{f}}}{K_{\mathrm{i}}}$ the ratio between the final $\kappa_{\mathrm{f}} = \sqrt{1 + \frac{g_{\mathrm{f}}}{\pi v_{\mathrm{F}}}}$ and the initial $\kappa_{\mathrm{i}} = \sqrt{1 + \frac{g_{\mathrm{i}}}{\pi v_{\mathrm{F}}}}$ Luttinger parameter. In this work, we focus on a zero-temperature initial state $n_{i,q} = 0$ for all q. The phonon density after the quench $n_{t,q} > 0$ is always larger than the density before the quench, resulting in a nonzero excitation energy $\Delta E = \langle H_{\mathrm{f}} \rangle - \langle H_{\mathrm{i}} \rangle > 0$ generated by the quench. Nonzero off-diagonal occupations $m_{t,q} \neq 0$ indicate that the correlations are not diagonal in the postquench quasiparticle basis and in order to relax to an equilibrium state, $m_{t,q}$ must decay to zero. In the present setting, we choose $m_{t,q} = e^{-2iu|q|t} \langle a_q^\dagger a_{-q}^\dagger \rangle_t$ such that the off-diagonal occupations remain always real, being either positive or negative, depending on the quench.

In the phonon basis,

$$H = \int_q u|q| a_q^\dagger a_q + \int_{q,k} \sqrt{|qk(k+q)|}\, v(k,q) (a_{q+k}^\dagger a_q a_k + \mathrm{H.c.}), \tag{2.8}$$

with the vertex function $v(k,q) = v(\frac{q}{|q|}, \frac{k}{|k|}, \frac{k+q}{|k+q|})$, which depends on the signs of the ingoing and outgoing momenta. In the interaction representation the phonon scattering Hamiltonian is

$$H_I(t) = \int_{q,k} \sqrt{|qk(k+q)|}\, v(k,q) \times (a_{q+k}^\dagger a_q a_k e^{iut(|q+k| - |q| - |k|)} + \mathrm{H.c.}). \tag{2.9}$$

Instead of solving the full problem, we aim at extracting the dominant contributions of the nonlinearity, which are relevant for intermediate and long times and which drive the crossover towards thermalization. In view of Eq. (2.9), off-resonance processes, for which $|q| + |k| \neq |k + q|$, will dephase and as a consequence become negligible for the intermediate- and long-time evolution of the system [47]. Resonant processes, on the other hand, here set by $|q| + |k| = |k + q|$, will at intermediate and long times become relevant in the renormalization-group sense, as discussed in Ref. [66]. The off-resonance processes can be eliminated perturbatively [66], yielding subleading corrections for intermediate and long times, which we will neglect in the following. For the asymptotic thermalization process, these subleading corrections will yield nonuniversal corrections (i.e., observable in microscopic constants and prefactors). For instance, the presence of off-resonance scattering events will eventually lower the asymptotic temperature compared to a system with purely resonant scattering events. The influence of off-resonance interactions on the decay rate of the bosonic and fermionic quasiparticles has been investigated in Ref. [59]. The decay rate extracted from this computation is orders of magnitude lower than the rate due to purely resonant scattering processes. Furthermore, it has a subleading scaling behavior $\sim T q^4$ compared to $\sim \sqrt{q^3 T}$ for resonant scattering processes at small momenta q [45,47]. Consequently, it is thus no influence on the leading-order long-time behavior. This allows us for the present purpose to restrict the phonon

scattering to the resonant processes alone:

$$H = \int_q u|q|a_q^\dagger a_q + v_0 \int'_{q,k} \sqrt{|qk(k+q)|}\,(a_{q+k}^\dagger a_q a_k + \text{H.c.}), \tag{2.10}$$

where the integral $\int'_{q,k}$ is performed for momenta $|q+k| = |q|+|k|$ and $v_0 = v(1,1) = \frac{3}{m}\sqrt{\frac{\pi}{K}}$ is the strength of the nonlinearity at resonance [47,57].

As we are interested in fermionic correlation functions, we switch from an operator-based formalism to a field-theoretic formulation on the Keldysh contour, which is explained in Appendix A; see also Ref. [57]. This allows us to treat both spatial and temporal forward-time correlations on an equal footing. We will focus our analysis on the so-called fermionic lesser Green's function

$$G^<_{t,x} = -i\,\langle \bar\psi_{t,x}\psi_{t,0}\rangle \tag{2.11}$$

at equal forward times t from which all fermionic equal-time correlations can be deduced. In particular, in terms of a physical interpretation, it is the Fourier transform of the fermionic momentum distribution

$$n^{\mathrm{F}}_{t,q} = i\int_x e^{iqx} G^<_{t,x}. \tag{2.12}$$

In the field theory representation, the bosonized fermionic lesser Green's function at equal times is

$$G^<_{\eta,t,x} = -i\,\langle \bar\psi_{\eta,-,t,x}\psi_{\eta,+,t,0}\rangle = -i\Lambda\frac{e^{-i\eta k_{\mathrm{F}}x}}{2\pi}e^{-(i/2)\mathcal{G}^<_{\eta,t,x}}. \tag{2.13}$$

Here $\bar\psi_\nu,\psi_\nu$ label Grassmann fields with the index $\nu = (\eta,\gamma,t,x)$ representing right and left movers ($\eta = \pm$), the contour variables on the Keldysh plus and minus contour ($\gamma = \pm$), the forward-time coordinate t, and the relative spatial distance x. The corresponding lesser exponent $\mathcal{G}^<$ is defined as

$$\mathcal{G}^<_{\eta,t,x} = 2i\,\ln\langle e^{i(\eta\phi_{+,t,0}-\theta_{+,t,0}-\eta\phi_{-,t,x}+\theta_{-,t,x})}\rangle. \tag{2.14}$$

The extra index $\pm$ of the Luttinger fields labels position on the plus-minus contour (see Appendixes A and B). Combining Eq. (2.14) and the Bogoliubov transformation above, one finds that $\mathcal{G}^<_{-\eta,t,x} = \mathcal{G}^<_{\eta,t,-x}$. The Green's function of the left movers is the spatially mirrored Green's function of the right movers and it is sufficient to consider only the Green's function of the right movers

$$G^<_{t,\eta x} \equiv G^<_{+,t,\eta x} = G^<_{\eta,t,x} \tag{2.15}$$

and equivalently for the exponent $\mathcal{G}^<$. According to the linked cluster theorem, the logarithm in Eq. (2.14) is defined as the sum of all connected diagrams in an expansion of the exponent. As a consequence, it can be expressed to leading order in terms of the full Green's functions, with the next nonvanishing correction being proportional to the equal-time one-particle irreducible four-point vertex, which is zero in the microscopic theory. Its effective correction remains negligibly small. In particular, the four-point vertex will only contribute to $\mathcal{O}((um)^{-4})$, which is two orders of magnitude smaller than the desired accuracy and its contribution can be safely neglected. The static one-particle irreducible four-point vertex represents a negligible correction for any equilibrium problem since it can only be generated via multiple concatenation of subleading three-point vertices. In particular, it is not responsible for the modifications of the dynamic structure factor reported in Refs. [49,50,52], since at zero temperature vertex corrections vanish exactly due to causality [57,67]. Consequently, the modifications of the dynamic structure factor happen entirely on the basis of the irreducible two-point vertex, i.e., the phonon self-energy. In the present case, the four-point vertex is exactly zero before the quench since this state corresponds to a zero-temperature state as well as immediately after the quench, since a flat quasiparticle distribution in Eq. (2.7) leads to a vanishing vertex correction. In terms of the Luttinger fields and apart from four-point vertex corrections, the exponent for the fermionic Green's function is

$$\mathcal{G}^<_{t,x} = \sum_{\alpha,\beta=\theta,\phi}(2\delta_{\alpha\beta}-1) \times\left[G^K_{\alpha\beta,t,0} - G^K_{\alpha\beta,t,x} + G^A_{\alpha\beta,t,x} - G^R_{\alpha\beta,t,x}\right], \tag{2.16}$$

where $G^{R/A}_{\alpha\beta}$ is the retarded, advanced Green's function for $\alpha,\beta = \theta,\phi$ and $G^K_{\alpha\beta}$ is the corresponding Keldysh Green's function, i.e., $G^R_{\alpha\beta,t,x} = -i\,\langle \alpha_{q,x,t}\beta_{c,0,t}\rangle$. Applying the Bogoliubov transformation to the phonon basis, the equal-time exponent becomes

$$\begin{aligned}\mathcal{G}^<_{t,x} = i\int_q\Bigg[&\frac{\pi e^{-|q|/\Lambda}}{|q|}[\cos(qx)-1]\\ &\times\left(\frac{K^2+1}{K}(2n_{t,q}+1) + 2\frac{K^2-1}{K}\cos(2u|q|t)m_{t,q}\right)\Bigg]\\ &+2\arctan(\Lambda x)\\ &+4i\int_q\left[\frac{\pi e^{-|q|/\Lambda}}{|q|}\sin(|q|x)\sin(2u|q|t)m_{t,q}\right].\end{aligned} \tag{2.17}$$

Here $n_{t,q} = \langle a^\dagger_{t,q}a_{t,q}\rangle$ and $m_{t,q} = |\langle a_{t,-q}a_{t,q}\rangle|$ are the equal-time normal and anomalous phonon densities, which evolve in time due to phonon scattering. The absence of the quasiparticle self-energy in this expression is caused by the equal-time properties of the Green's function and underlines the fact that time local, i.e., static, observables, even if explicitly forward-time dependent, are not modified by the frequency-resolved fine structure of the self-energies once the time-dependent distribution $n_{t,q}$ is known. In the remainder of this paper, we will analyze the time evolution of the exponent (2.17) after the interaction quench and its implications for the fermionic Green's function (2.13).

Concerning the relevance of the interacting Luttinger model, before closing the section, we would like to mention that only recently pioneering experiments in ultracold gases both in and out of equilibrium explored the transient and prethermalization dynamics of systems [16–26,68–70] effectively described by a quadratic Luttinger model, the bosonic theory of the Hamiltonian in Eq. (2.2). In particular, in Refs. [16–18,24] prethermal states in the relative phase of a suddenly split condensate have been identified that have been stable on the experimentally accessible time scales. For the latter experiments, the cubic nonlinearity studied in the present work constitutes the leading-order correction to

the quadratic theory in a gradient expansion. Therefore, the framework developed in the subsequent sections to describe the relaxation dynamics in the system is of direct experimental relevance once the time scales are experimentally accessible to study the escape out of the prethermalization plateau. It is important, however, to note that the concrete experimental setup of the suddenly split condensate requires a further but straightforward extension of the considered model system to include two species of coupled bosonic fields. Moreover, let us emphasize that these experimental systems do not simulate the Luttinger liquid of interacting fermions—our initial motivation—but directly simulate the effective bosonic low-energy theory. In this way, it might be possible to obtain experimental access to the dynamics of the bosonic occupation distributions, governed by the kinetic theory formulated below, via time-of-flight imaging.

III. SUMMARY OF MAIN RESULTS

Before formulating and solving the kinetic theory for the interacting Luttinger liquid in detail, we briefly summarize the main results reported in this work. In the subsequent sections, we will then present the detailed calculations. Specifically, the known results on the purely integrable system are reformulated within the present framework in Sec. IV B. The kinetic equation, used to address the presence of the nonlinear phonon scattering, is derived in Sec. V. This kinetic equation is then solved in Sec. VI.

It is the aim of this work to study the thermalization dynamics of the fermionic equal-time Green's function (2.11), which is the Fourier transform of the fermionic momentum distribution (2.12) and contains the information on quadratic equal-time fermion observables. Without loss of generality, we focus on the distribution of the right movers, i.e., $\eta = +$. In the presence of phonon scattering, we determine the time evolution of $G^<_{t,x}$ via a set of kinetic equations derived later in Sec. V.

We find that $G^<_{t,x}$ features two distinct spatiotemporal crossover scales $x_{\rm th}(t)$ and $x_{\rm pt}(t)$, separating three regimes with distinct scaling behavior:

$$\begin{aligned} &x_{\rm pt}(t) \ll |x| \quad \text{(prequench)},\\ &x_{\rm th}(t) \ll |x| \ll x_{\rm pt}(t) \quad \text{(prethermal)},\\ &|x| \ll x_{\rm th}(t) \quad \text{(thermal)}. \end{aligned}$$

We find for the associated crossover scales $x_{\rm pt}(t)$ and $x_{\rm th}(t)$,

$$x_{\rm pt}(t) = 2ut, \quad x_{\rm th}(t) = \frac{x_\lambda}{\Lambda}(v_0\Lambda^2 t)^{\alpha_\lambda}. \tag{3.1}$$

The first crossover at $x_{\rm pt}(t)$ determines the light cone [7] set by the sound velocity u of the phononic elementary excitations and is known from the noninteracting Luttinger model. Two space points a distance $x \gg x_{\rm pt}(t)$ apart from each other have not been able to exchange information after the quench due to causality. Therefore, the properties at such distances are solely given by the initial condition before the quench such that we term this regime prequench. For distances $x < x_{\rm pt}$ quasiparticles are starting to form, marking the onset of prethermalization. The second crossover takes place at $x = x_{\rm th}(t)$ setting the scale for the onset of thermalization due to quasiparticle scattering. The exponent α_λ with $0 < \alpha_\lambda < 1$, as well as the dimensionless length x_λ, depends on the quench parameter λ only and can be determined numerically. The upper bound of α_λ is guaranteed by the subleading nature of the vertex, which forbids ballistic spreading in the thermal region. The treatment of quasiparticle scattering in terms of a kinetic equation approach is only valid on distances for which a well-defined prethermal plateau has been established. Given this, we estimate the kinetic equation approach to be valid on distances

$$x < x_c(t) = x_{\rm th}(t)\exp\left(-\frac{K^2+1}{|K^2-1|}\sqrt{\frac{3n_\lambda}{|m_\lambda|}}\right) \tag{3.2}$$

and in the scatterless region $x > x_{\rm th}$. In the intermediate regime $x_c(t) < x < x_{\rm th}$, quasiparticle scattering is as fast as the formation of quasiparticles such that both effects have no distinguishable time scale. While the results obtained from our approach might not be reliable in this region, $x_{\rm th}(t)$ remains the crossover scale below which the nonlinearity becomes non-negligible. The fact that $x_{\rm th}(t)$ has an explicit dependence on the Luttinger cutoff Λ ($\alpha_\lambda > 1/2$ generally) is not surprising. The nonlinearity in the Luttinger model introduces a microscopic energy scale $v_0\Lambda^2$ that represents the characteristic time scale of the dynamics induced by the nonlinearity, i.e., in the present case the thermalization dynamics beyond the quadratic theory. Additionally, the nonlinearity breaks the scale invariance of the quadratic model, which is responsible for the fact that all microscopic scales can be eliminated from macroscopic observables in that case. In the absence of scale invariance, however, the microscopic length scale Λ will appear in certain observables, expressing that their explicit value depends on model specific details.

As we show in our detailed analysis below, we find that this separation into three spatiotemporal regimes, prequench, prethermal, and thermal, reflects itself in a remarkable factorization property of the Green's function

$$G^<_{t,x} = G^<_{0,x} Z_{\rm pt}(s_{\rm pt}) Z_{\rm th}(s_{\rm th}), \tag{3.3}$$

which holds everywhere except in the vicinity of the crossover scales $x_{\rm th}(t)$ and $x_{\rm pt}(t)$. Here we have introduced the following shorthand notation:

$$\begin{aligned} s_{\rm pt} &= \begin{cases} clx & \text{for } x < x_{\rm pt}(t)\\ 2ut & \text{for } x > x_{\rm pt}(t), \end{cases}\\ s_{\rm th} &= \begin{cases} x & \text{for } x < x_{\rm th}(t)\\ x_{\rm th}(t) & \text{for } x > x_{\rm th}(t). \end{cases} \end{aligned} \tag{3.4}$$

While the factorization into $G^<_{0,x}$ and $Z_{\rm pt}$ is already known for the exact solution of the integrable model [6], here we show that the influence of the nonlinearity can be captured by a further factor in terms of $Z_{\rm th}$. The thermal contribution $Z_{\rm th}(s_{\rm th})$ exhibits interesting spatiotemporal dynamics in particular in the long-time regime $ut \gg x_{\rm th}(t)$. It is defined as

$$Z_{\rm th}(s_{\rm th}) = \exp\left(-\frac{K^2+1}{K}\frac{\pi \tilde{T}_t |s_{\rm th}|}{u}\right) \tag{3.5}$$

and features two different spatiotemporal regimes.

(i) Thermalized regime. Deep in the thermalized region $|x| \ll x_{\rm th}(t)$, where $s_{\rm th} = x$, $Z_{\rm th} = \exp(-|x|/\xi_{\tilde{T}_t})$ exhibits the

conventional exponential decay with distance that the system experiences in thermal states with an associated thermal length

$$\xi_{\tilde{T}_t} = \frac{K}{1+K^2}\frac{u}{\pi \tilde{T}_t}. \tag{3.6}$$

The effective temperature $\tilde{T}_t$, however, entering this equation remains a dynamical quantity with

$$\tilde{T}_t = T + u\Lambda\Delta_\lambda(v_0\Lambda^2 t)^{-\mu}, \tag{3.7}$$

approaching the temperature T of the final thermal ensemble algebraically slowly. We find that the numerical simulations of the kinetic equation are consistent with an analytical estimate for the exponent $\mu = 2/3$. Thus, the system in this spatial region appears to be hotter than in the final asymptotic thermal state. The associated excess energy stored at short distances has to be transported to larger distances, which, however, is an algebraically slow process since this energy transport in the presence of detailed balance is carried out by dynamical slow modes, emerging as a consequence of exact conservation laws [71].

(ii) Prethermal and prequench regime. Within the prethermal and prequench region $x_{\rm th}(t) \ll x$, the amplitude $Z_{\rm th}(s_{\rm th}) = Z_{\rm th}[x_{\rm th}(t)]$ approaches a space-independent but time-dependent constant quantifying the temporal decay of the prethermal correlations:

$$Z_{\rm th}[x_{\rm th}(t)] = \exp[-x_{\rm th}(t)/\xi_{\tilde{T}_t}]. \tag{3.8}$$

Because $x_{\rm th}(t) \propto (v_0\Lambda^2 t)^{\alpha_\lambda}$, we have, remarkably, that this amplitude decays in stretched exponential form. This decay is subexponential and thus inherently nonperturbative in nature, highlighting the capabilities of our present approach.

IV. DYNAMICS IN THE ABSENCE OF PHONON SCATTERING

In order to systematically understand the effect of phonon scattering on the relaxation dynamics after the interaction quench, we first determine the dynamics of the exponent $\mathcal{G}^<_{t,x}$ in the absence of scattering, i.e., for $\frac{1}{m}, v_0 \to 0$. This quench scenario has been extensively discussed in Refs. [6,12,13,72,73] and we will only briefly list the known results in the present formalism in order to make a connection with the relaxation dynamics in the presence of phonon scattering, which are discussed subsequently.

A. Ground-state properties

For a system in the ground state, $n_{t,q} = m_{t,q} = 0$ and the exponent evaluates to

$$\mathcal{G}^<_{t,x} = -i\frac{K^2+1}{2K}\ln(1+\Lambda^2x^2) + 2\arctan(\Lambda x), \tag{4.1}$$

which leads to a time-independent fermionic Green's function

$$G^<_{t,x} = -\frac{i\Lambda}{2\pi}e^{-ik_{\rm F}x - i\arctan(\Lambda x)}\sqrt{1+\Lambda^2x^2}^{-(K^2+1)/2K}, \tag{4.2}$$

well known from the literature [9,11]. It features an algebraic decay in space $\sim x^{-(K^2+1)/2K}$ and a power-law singularity of the fermionic momentum distribution close to the Fermi momentum $n^{\rm F}_q \sim |q-k_{\rm F}|^{-(K-1)^2/2K}$ [11].

B. Quench from the ground state

Initializing the fermions in the ground state and performing an interaction quench leads to constant nonzero phonon densities in the postquench basis, according to Eq. (2.7). In the absence of scattering, the phonon densities are constants of motion and remain time independent, $n_{t,q} = n_{0,0} \equiv n$ and $m_{t,q} = m_{0,0} \equiv m$. In this situation, only dephasing of the off-diagonal Green's functions induces relaxation and the exponent is

$$\begin{aligned}\mathcal{G}^<_{t,x} &= 2\arctan(\Lambda x) - i\frac{K^2+1}{2K}(2n+1)\ln(1+\Lambda^2x^2) + im\ln\left(\frac{1+\Lambda^2(x-2ut)^2}{1+\Lambda^2(x+2ut)^2}\right)\\ &\quad - i\frac{K^2-1}{2K}m\left[\ln\left(\frac{1+\Lambda^2(x-2ut)^2}{1+4u^2t^2\Lambda^2}\right) + \ln\left(\frac{1+\Lambda^2(x+2ut)^2}{1+4u^2t^2\Lambda^2}\right)\right]\\ &= \mathcal{G}^<_{0,x} + im\ln\left(\frac{1+\Lambda^2(x-2ut)^2}{1+\Lambda^2(x+2ut)^2}\right) - i\frac{K^2-1}{2K}m\ln\left[\frac{(1+\Lambda^2(x+2ut)^2)(1+\Lambda^2(x-2ut)^2)}{(1+4u^2t^2\Lambda^2)^2(1+x^2\Lambda^2)^2}\right].\end{aligned} \tag{4.3}$$

Here $\mathcal{G}^<_{0,x}$ is the exponent corresponding to the prequench state, i.e., the ground state of interacting fermions with the prequench Luttinger parameter K_i. Consequently, the fermion Green's function (2.13) factorizes

$$G^<_{t,x} = G^<_{0,x}\tilde{Z}_{\rm pt}(x,t). \tag{4.4}$$

The factor $\tilde{Z}_{\rm pt}$ is defined by Eqs. (4.3) and (2.13) and describes the time-dependent modification of the initial zero-temperature Green's function due to the quench. In view of the following discussion it is useful to investigate this factor for distances away from the light cone $x = 2ut$. For distances $|x| \ll 2ut$, the temporal factors in Eq. (4.3) cancel each other and $\tilde{Z}_{\rm pt}(t,x) \overset{|x|\ll 2ut}{\longrightarrow} Z_{\rm pt}(x)$ loses its time dependence. On the other hand, for distances $|x| \gg 2ut$, the spatial dependence drops out and $\tilde{Z}_{\rm pt}(t,x) \overset{|x|\gg 2ut}{\longrightarrow} Z_{\rm pt}(2ut)$. This defines the prethermal amplitude

$$Z_{\rm pt}(s) = (\sqrt{1+\Lambda^2s^2})^{[(K^2-1)/2K][(1-\lambda^2)/4\lambda]}. \tag{4.5}$$

The process associated with the crossover of $Z_{\rm pt}(s)$ from a temporal to a spatial dependence as a function of time is the formation of quasiparticles corresponding to the postquench

Hamiltonian. This is the typical prethermalization scenario in the absence of quasiparticle scattering. For short times, the properties of the system are dominated by the initial state of the system and the fermion Green's function is only modified by a global amplitude but has the same spatial scaling behavior as for the initial state. The effect of the quadratic Hamiltonian in the time evolution is the dephasing of all terms, which are not diagonal in the basis of the postquench quasiparticles, leading to a diagonal ensemble in the quasiparticles with a nonequilibrium phonon density. This nonequilibrium distribution of phonons induces a scaling behavior of the fermion Green's function in real space, which is different from the zero- and finite-temperature cases.

In the absence of phonon scattering, the diagonal phonon densities $n_{t,q}$ are constants of motion and do not relax; the density matrix ρ therefore does not approach a Gibbs state but is rather described in the asymptotic limit $t \to \infty$ by a GGE, which respects the constants of motion and maximizes the entropy. It is given by

$$\rho_{\mathrm{GGE}} = Z_{\mathrm{GGE}}^{-1} \exp\left(-\int_q \nu_q \hat{n}_q\right), \tag{4.6}$$

where the Lagrange parameters $\nu_q = 2\ln(\frac{\lambda+1}{|\lambda-1|})$ depend on the quench parameter and Z_{GGE} is the normalization factor.

The fermion Green's function for the two different regimes is then

$$G^<_{t,x} = G^<_{0,x} \times \begin{cases} Z_{\mathrm{pt}}(2ut) & \text{for } |x| \gg 2ut \\ Z_{\mathrm{pt}}(x) & \text{for } |x| \ll 2ut, \end{cases} \tag{4.7}$$

with the nonequilibrium scaling behavior

$$G^<_{t,x} \overset{t\to\infty}{\sim} |x|^{-\gamma_{\mathrm{Eq}}\gamma_{\mathrm{GGE}}}, \tag{4.8}$$

where $\gamma_{\mathrm{eq}} = \frac{K^2+1}{2K}$ is the equilibrium exponent and $\gamma_{\mathrm{GGE}} = \frac{\lambda^2+1}{2\lambda} = 2n+1$ [see Eq. (2.7)] is the nonequilibrium correction resulting from a nonthermal quasiparticle distribution.

V. PHONON SCATTERING AND THE KINETIC EQUATION

In the preceding sections, we have demonstrated that the forward-time evolution of the fermionic equal-time Green's function can be determined solely from the momentum-dependent excitation distributions $n_{t,q}$,$m_{t,q}$. All quadratic equal-time observables, on the other hand, can be computed from the fermionic equal-time Green's function via a unitary transformation such that the knowledge of $n_{t,q}$ and $m_{t,q}$ gives access to the forward-time evolution of all the frequency-independent quadratic fermion observables. Therefore, the time evolution of this specific set of observables can be captured by the time evolution of the frequency-independent and well-defined quantities $n_{t,q}$,$m_{t,q}$, which does not necessitate the frequency-resolved fine structure in the fermionic spectrum. In order to determine the time evolution of the phonon densities, we derive kinetic equations for the excitation distribution function [54] in the limit of well-defined excitations, closely following the steps in Ref. [57] and briefly discussing the approximations.

Before we start with the explicit derivation, we review very briefly the known results for nonlinear Luttinger liquids (see [64]) and place the present approach in this context. At zero temperature and without band curvature, long-wavelength physics of the interacting fermion model can be exactly mapped to the quadratic Luttinger model and therefore has well-defined sharp phononic excitations, expressed by a spectral function of the phonons $\mathcal{A}_{q,\omega} = i(G^R_{q,\omega} - G^A_{q,\omega}) = 2\pi\delta(\omega - u|q|)$. In the presence of band curvature, however, the phonons themselves interact via a resonant three-point scattering vertex, which leads to a broadening of the spectral function around the mass shell $\omega = u|q|$. This broadening can be described in terms of two excitations branches at frequencies $\omega = \epsilon^{\pm}_q$, where $\epsilon^-_q < u|q|$ labels a solitonic branch and $\epsilon^+_q > u|q|$ labels a phononic branch (such that $|\epsilon^+_q - \epsilon^-_q|/q \to 0$ for $q \to 0$) [52,64]. The spectral weight of the excitations in the nonlinear Luttinger liquid is distributed continuously between these two branches. Whereas the solitonic branch represents an exact boundary (i.e., no spectral weight is located at frequencies $\omega < \epsilon^-_q$), featuring a power-law singularity for frequencies above ϵ^-_q, the phononic branch represents an algebraically sharp boundary (i.e., the spectral weight for frequencies $\omega > \epsilon^+_q$ is strongly algebraically suppressed), featuring a power-law singularity from both sides [64]. While the power-law singularities at the edges of the spectral weight obviously cannot be explained by a frequency-independent self-energy, the characteristic width of the spectral weight $\delta\omega_q = \epsilon^+_q - \epsilon^-_q = \frac{q^2}{m^*}$ can be captured by an imaginary part of the on-shell value of the self-energy $\Sigma^R_{q,\omega=u|q|}$, which determines the renormalized mass m^* [47,52,64,65]. These results hold for the zero-temperature limit of the problem. At finite temperature $T > 0$, however, a self-consistent Born approximation for the on-shell self-energy predicts a scaling of the spectral weight $\delta\omega_q \sim \sqrt{|q|^3 T}$ [74,75], which has also been observed in numerical simulations of interacting one-dimensional bosons [74]. For $\delta\omega_q \ll u|q|$, i.e., the width of the spectral weight of the excitations being much smaller than the average excitation energy, the spectral weight is still sharply concentrated at the mass shell and one can still think of (physically) well-defined excitations, although the fine structure of the spectral weight is very different from what one is used to for weakly interacting quasiparticles. As a consequence, it is possible to derive a kinetic equation for the excitation densities in this regime, applying the common quasiparticle and local time approximations, and we will implement this approach below. It neglects the specific structure of the spectral weight of nonlinear Luttinger liquids, which is valid for static variables in the quasiparticle limit $\delta\omega_q \ll u|q|$. We begin by introducing the interaction picture for the Heisenberg operators

$$\bar{a}_{t,q} \to \bar{a}_{t,q} e^{-iu|q|t}, \tag{5.1}$$

which leaves the Hamiltonian (2.10) unmodified but shifts the spectral weight of diagonal modes to zero frequency and eliminates the phase $\sim e^{i2u|q|t}$ of off-diagonal correlation functions [57]. The Green's functions in the interaction representation are labeled with a tilde. The Keldysh Green's function in Nambu space is

$$i\tilde{G}^K_{t,q,\delta} = \begin{pmatrix} \langle\{a_{t+\delta/2,q}, \bar{a}_{t-\delta/2,q}\}\rangle & \langle\{a_{t+\delta/2,q}, a_{t-\delta/2,-q}\}\rangle \\ \langle\{\bar{a}_{t+\delta/2,-q}, \bar{a}_{t-\delta/2,q}\}\rangle & \langle\{\bar{a}_{t+\delta/2,q}, a_{t-\delta/2,q}\}\rangle \end{pmatrix}, \tag{5.2}$$

where $\{\cdot,\cdot\}$ is the anticommutator and we introduced an additional relative time shift δ associated with spectral properties of the system. The retarded Green's function is

$$i\tilde{G}^R_{t,q,\delta} = \theta(\delta)\begin{pmatrix} \langle[a_{t+\delta/2,q},\bar{a}_{t-\delta/2,q}]\rangle & \langle[a_{t+\delta/2,q},a_{t-\delta/2,-q}]\rangle \\ \langle[\bar{a}_{t+\delta/2,-q},\bar{a}_{t-\delta/2,q}]\rangle & \langle[\bar{a}_{t+\delta/2,q},a_{t-\delta/2,q}]\rangle \end{pmatrix} = \theta(\delta)\begin{pmatrix} \langle[a_{t+\delta/2,q},\bar{a}_{t-\delta/2,q}]\rangle & 0 \\ 0 & \langle[\bar{a}_{t+\delta/2,q},a_{t-\delta/2,q}]\rangle \end{pmatrix}. \tag{5.3}$$

The off-diagonal retarded and advanced Green's functions are exactly zero. This is a consequence of the Hamiltonian, which does not introduce a coupling between the modes q and $-q$, such that the commutator $[a_{t+\delta/2,q},a_{t-\delta/2,-q}] = 0$ for all times t,δ. The anti-Hermitian Keldysh Green's function is parametrized according to [54,57]

$$\tilde{G}^K_{t,q,\delta} = (\tilde{G}^R \circ \sigma_z \circ F - F \circ \sigma_z \circ \tilde{G}^A)_{t,q,\delta} \tag{5.4}$$

in terms of the time-dependent Hermitian quasiparticle distribution function F and the Pauli matrix σ_z, the latter preserving the symplectic structure of bosonic Nambu space. The $\circ$ represents matrix multiplication with respect to momentum space and convolution with respect to time. Switching to Wigner coordinates by Fourier transforming the Keldysh Green's function with respect to relative time

$$\tilde{G}^K_{t,q,\omega} = \int_\delta \tilde{G}^K_{t,q,\delta} e^{i\omega\delta} \tag{5.5}$$

and applying the Wigner approximation, which, due to the RG-irrelevant interactions, is justified in the same regime for which the Luttinger description is applicable [57,76], we find

$$\tilde{G}^K_{t,q,\omega} = \tilde{G}^R_{t,q,\omega}\sigma_z F_{t,q,\omega} - F_{t,q,\omega}\sigma_z \tilde{G}^A_{t,q,\omega}, \tag{5.6}$$

which is diagonal in momentum and frequency space. Inverting Eq. (5.6) by multiplying it with $(\tilde{G}^R)^{-1}$ from the left and $(\tilde{G}^A)^{-1}$ from the right yields the kinetic equation for the distribution function

$$i\partial_t F_{t,q,\omega} = \sigma_z \Sigma^R_{t,q,\omega} F_{t,q,\omega} - F_{t,q,\omega}\Sigma^A_{t,q,\omega}\sigma_z - \sigma_z \Sigma^K_{t,q,\omega}\sigma_z. \tag{5.7}$$

The retarded, advanced self-energies $\Sigma^{R/A}_{t,q,\omega}$ are diagonal in Nambu space, while the Keldysh self-energy $\Sigma^K_{t,q,\omega}$ consists of nonvanishing diagonal and off-diagonal entries due to the initial off-diagonal occupations $m_{0,q} \neq 0$.

The kinetic equation for the phonon occupations is obtained by multiplying Eq. (5.7) on both sides with the spectral function $\tilde{\mathcal{A}}_{t,q,\omega} = i(\tilde{G}^R_{t,q,\omega} - \tilde{G}^A_{t,q,\omega})$ and integrating over frequency space. For interacting Luttinger liquids, the spectral function $\tilde{\mathcal{A}}_{t,q,\omega}$ is very narrowly peaked at the mass shell and the kinetic equation is essentially locked onto $\omega = 0$ in this way (in the interaction picture, the mass shell is at $\omega = 0$). As a consequence, one finds kinetic equations for the diagonal densities

$$\partial_t n_{t,q} = -\sigma^R_{t,q}(2n_{t,q}+1) + \sigma^K_{t,q} \tag{5.8}$$

and the off-diagonal densities

$$\partial_t m_{t,q} = -2\sigma^R_{t,q} m_{t,q} - \Gamma^K_{t,q}. \tag{5.9}$$

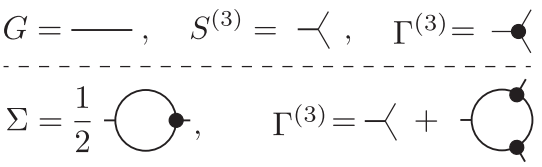

FIG. 2. Diagrammatic illustration of the Dyson-Schwinger equations up to cubic order. Here G represents the full Green's function, $S^{(3)}$ the bare three-body vertex, and $\Gamma^{(3)}$ the full three-body vertex. For convenience, this displays only the topology of the diagrams, which has not been extended to Keldysh space.

They can be expressed in terms of the imaginary part of the retarded on-shell self-energy

$$\sigma^R_{t,q} = \frac{1}{2}\int_\omega \tilde{\mathcal{A}}_{t,q,\omega}\left(\Sigma^R_{t,q,\omega} - \Sigma^A_{t,q,\omega}\right) \approx \frac{1}{2}\left(\Sigma^R_{t,q,\omega=0} - \Sigma^A_{t,q,\omega=0}\right) \tag{5.10}$$

and the Keldysh on-shell self-energies

$$\sigma^K_{t,q} = \frac{i}{2}\int_\omega \tilde{\mathcal{A}}_{t,q,\omega}\left(\Sigma^K_{t,q,\omega}\right)_{11} \approx \frac{i}{2}\left(\Sigma^K_{t,q,\omega=0}\right)_{11} \tag{5.11}$$

and

$$\Gamma^K_{t,q} = \frac{i}{2}\int_\omega \mathcal{A}_{t,q,\omega}\left(\Sigma^K_{t,q,\omega}\right)_{12} \approx \frac{i}{2}\left(\Sigma^K_{t,q,\omega=0}\right)_{12}. \tag{5.12}$$

The Keldysh self-energy is always anti-Hermitian and therefore purely imaginary in frequency and momentum space, such that Eqs. (5.8) and (5.9) are real. Since the criterion $|\epsilon^+_q - \epsilon^-_q| \ll u|q|$ is equivalent to $\sigma^R_{t,q} \ll u|q|$ at zero- and finite-temperature equilibrium, we also apply the latter criterion for the present out-of-equilibrium situation in order to estimate the validity of our approach.

The phonon scattering terms in Eq. (2.10) are resonant, i.e., they describe scattering between a continuum of energetically degenerate states, and as a consequence, perturbation theory diverges. In order to determine the self-energies $\sigma^R_{t,q},\sigma^K_{t,q},\Gamma^K_{t,q}$, we apply nonperturbative Dyson-Schwinger equations, which are truncated at cubic order. This takes into account renormalization effects of the cubic vertex and yields nonperturbative self-energies. The topology of the corresponding diagrams is shown in Fig. 2. If we neglect the cubic vertex correction, the Dyson-Schwinger equations reduce to the self-consistent Born approximation [57]. For an initial state with constant phonon density, as is the case for the present setup, the vertex correction has been shown to be exactly zero [57,67]; however, it obtains a nonzero value in the time evolution of the system. The kinetic equations (5.8) and (5.9) are solved iteratively, starting at a certain time t, and the self-energies and vertex correction are computed as functions of the distributions $n_{t,q},m_{t,q}$. Subsequently $\partial_t n_{t,q},\partial_t m_{t,q}$ are determined and used in turn to compute the distributions $n_{t+\Delta,q},m_{t+\Delta,q}$ for an infinitesimally later time. This procedure is repeated in order to determine the time evolution of the phonon densities and self-energies. A more detailed technical derivation of the iterative solution for the kinetic equation, self-energies, and vertex correction can be found in Ref. [57].

VI. THERMALIZATION AND PRETHERMALIZATION DYNAMICS

As one can see from the kinetic equations (5.8) and (5.9), the diagonal and off-diagonal phonon densities are no longer constants of motion in the presence of phonon scattering and energy is redistributed between the different momentum modes. On a general level, when the system thermalizes, as we will show below, the steady state of the dynamics in the presence of a cubic scattering as in Eq. (2.10) is solely determined by the associated temperature T and independent of any further details of the initial nonequilibrium state. Specifically, the diagonal modes acquire a Bose-Einstein distribution $n_{\infty,q} = n_{t\to\infty,q} = (e^{u|q|/T} - 1)^{-1}$, whereas the off-diagonal distributions $m_q = 0$ have to vanish.

Importantly, in the resonant approximation, the final temperature T ($k_B = 1$ in the following) can be computed directly from the initial state as will be shown now. In a closed system, the total energy is conserved. Moreover, the conservation of the kinetic energy is an additional exact feature of the derived kinetic equation. As a consequence, also the interaction energy itself is individually conserved. The latter is not an artifact of the kinetic equation but a feature of the resonant nature of the interactions, which, by definition of resonance, commute with the quadratic part of the Hamiltonian (2.10) already on an operator level. This implies that the relaxation dynamics due to the interactions takes place in closed subsets of degenerate eigenstates of the quadratic Hamiltonian, which would, in the absence of phonon scattering, only acquire a global phase and would not be able to thermalize. Consequently, the kinetic energies of the initial (e_0) and final (e_f) states have to be equal, which yields

$$e_0 = u n_\lambda \Lambda^2 = \int_q u|q| n_{0,q} \stackrel{!}{=} \int_q u|q| n_{\infty,q} = \frac{T_\lambda^2 \pi^2}{3u} = e_f. \tag{6.1}$$

Here $n_{0,q}$ is the initial momentum distribution [see Eq. (2.7)] and $n_{\infty,q} = (e^{\beta u|q|} - 1)^{-1}$ is the final thermal distribution. This gives

$$T_\lambda = \frac{u\Lambda}{\pi}\sqrt{3n_\lambda}, \tag{6.2}$$

which depends on the details of the quench only through the quench parameter λ such that we denote the temperature via T_λ in the following. Importantly, this temperature yields a criterion for the applicability of the Luttinger theory for the present quench scenario, since Luttinger theory is only well defined for temperatures lower than the cutoff $T_\lambda < u\Lambda$. Evaluating this inequality results in a bound for the quench parameter λ, i.e., for $\frac{1}{15} \leqslant \lambda \leqslant 15$, the quench can be described in the framework of Luttinger theory.

In the remainder of this section, we will discuss the time evolution of the phonon densities according to the kinetic equation and derive the form of the Green's function in Eq. (3.3).

A. Phonon densities

The time evolution of the phonon densities is determined by the kinetic equations (5.8) and (5.9). In order to make the time evolution of the phonon densities dimensionless, we rescale the self-energy according to $\tilde{\sigma}^{R,K} = \frac{\sigma^{R,K}}{v_0\Lambda^2}$, the momentum $\tilde{q} = \frac{q}{\Lambda}$, and time $\tau = v_0\Lambda^2 t$. In these units, the time-evolved phonon densities depend only on the initial state and are independent of the microscopic details of v_0 and Λ [57], i.e., in the present setting the time evolution of the phonon density is completely determined by the quench parameter λ, which characterizes the initial state. Additionally, as a consequence of Eq. (2.7), the dynamics remains invariant under $\lambda \to 1/\lambda$ and $m_{\tau,q} \to -m_{\tau,q}$ and we therefore consider only the case $\lambda > 1$.

The time evolution of the phonon densities for three different quench parameters λ is shown in Fig. 3. It features two characteristic regimes, which are separated by a time-dependent crossover momentum $q_{\rm th}(\tau)$, which turns out to be the inverse thermal length scale $x_{\rm th}(\tau) = 1/q_{\rm th}(\tau)$. According to the numerical simulations, $q_{\rm th}(\tau)$ can be parametrized as $q_{\rm th}(\tau) = Q_\lambda \tau^{\alpha_\lambda}$, where the exponent α_λ and the amplitude Q_λ are monotonic functions of the quench parameter (for $\lambda > 1$). According to Fig. 3, away from the crossover, the phonon distribution can be written as

$$n_{\tau,q} = \begin{cases} n_\lambda + c_{\tau,\lambda}|q| & \text{for } |q| < q_{\rm th}(\tau) \\ \frac{\tilde{T}_{\tau,\lambda}}{u|q|} & \text{for } |q| > q_{\rm th}(\tau). \end{cases} \tag{6.3}$$

For small momenta $|q| < q_{\rm th}$, the phonon density increases linearly in momentum, with a time-dependent prefactor $c_{\tau,\lambda}$, which has to be computed numerically but is determined solely by the quench parameter. This linear increase is guaranteed by the structure of the cubic vertex, which induces a scaling of the one-loop diagrams $\sim|q|$ for small momenta q. This scaling is imposed by the U(1) symmetry of the action, which forbids a smaller exponent in the scaling of the local vertex as discussed in Ref. [57], where the same scaling behavior was found, although with a different amplitude c_τ reflecting the driven nature of the system in that case. The very same mechanism guarantees the pinning of the distribution at $q = 0$ to its initial value $n_{t,q=0} = n_{t=0,q=0}$, expressed by the constant n_λ in Eq. (6.3).

For larger momenta $|q| > q_{\rm th}$ fast quasiparticle scattering events have established a local equilibrium and the phonon density is well described by a Bose distribution function $n_{\rm B}(u|q|, \tilde{T}_{\tau,\lambda}) = (e^{u|q|/\tilde{T}_{\tau,\lambda}} - 1)^{-1}$, which can be approximated by a classical Rayleigh-Jeans distribution, as in Eq. (6.3), for intermediate momenta $q_{\rm th} < q < \frac{\tilde{T}_{\tau,\lambda}}{u}$. The effective temperature $\tilde{T}_{\tau,\lambda}$ approaches the final temperature $T_\lambda = \tilde{T}_{\tau\to\infty,\lambda}$ asymptotically, following a power law $\tilde{T}_{\tau,\lambda} - T_\lambda \sim \tau^\mu$, consistent with $\mu = 2/3$ for large times (see Sec. VI C). An important exception is represented by the $q = 0$ mode, which does not thermalize. The thermal momentum scale $q_{\rm th} \sim \tau^{-\alpha_\lambda}$ is larger than zero for any finite time $\tau < \infty$. As a consequence, for any realistic experiment, there will always exist a small momentum window $q \in [0, q_{\rm th}(t_{\rm max})]$, which does not thermalize during the run-time of the experiment $t_{\rm max}$. However, even in the limit $\tau \to \infty$, $n_{\tau,q=0}$ is pinned to its initial value by the exact U(1) symmetry of the fermionic system. This symmetry corresponds to the exact particle-number conservation of the fermionic theory. The occupation $n_{\tau,q=0}$ of the zero-momentum mode is directly related to the variance of the total particle number $n_{\tau,q=0} \sim \langle \hat{N}^2 \rangle_\tau - \langle \hat{N} \rangle_\tau^2$, where $\hat{N}$ is the

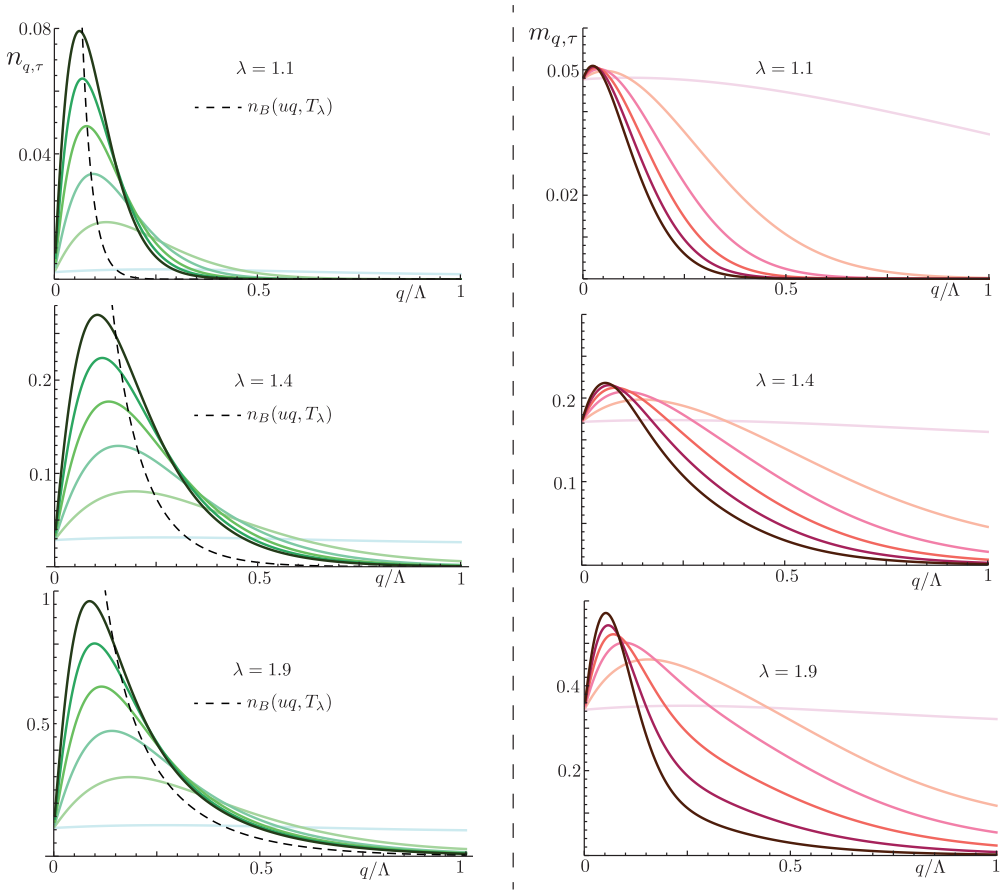

FIG. 3. Simulation of the time evolution of the diagonal phonon density $n_{\tau,q}$ (left column) and off-diagonal density $m_{\tau,q}$ (right column) for different quench parameters λ. In each row, the individual lines correspond to different times $\tau = (0,1,2,3,4,5)$. In the left column the total phonon density increases in time (from light to dark green) and the dotted lines represent the corresponding asymptotic density in the limit $\tau \to \infty$, which is a Bose distribution with the quench dependent temperature $T_\lambda = (0.035,0.124,0.24)u\Lambda$ (from the top to the bottom row). The distribution function is separated into two regimes according to Eq. (6.3), with a linear increase in momentum for small momenta and a corresponding thermal distribution for larger momenta. The crossover momentum separating the two regimes is marked with a dot. In the right column the off-diagonal phonon density is decreasing in time (from light to dark red), displaying two distinct momentum regimes: For momenta larger than the crossover $q > q_{\rm th}$, the off-diagonal occupation decreases exponentially in momentum, while it remains close to its initial value $m_{0,q} = m_\lambda$ for momenta smaller than the crossover. While any momentum mode $n_{\tau,q>0}$ will thermalize at a finite time $\tau < \infty$, the zero-momentum mode remains pinned to its initial value $n_{\tau,q=0} = n_{\tau=0,q=0}$. The latter is not an artifact of the approximation but a consequence of exact fermionic particle number conservation, as outlined in the main text.

total fermionic number operator [76,77]. For particle-number-conserving dynamics, it is therefore an integral of motion. Consequently, the asymptotic bosonic distribution function in the limit $\tau \to \infty$ is a perfect Bose-Einstein distribution, with a discontinuity at $q = 0$.

In order to express the factor $c_{\tau,\lambda}$ in terms of the temperature $\tilde{T}_{\tau,\lambda}$, we equate both forms of the distribution function $n_{\tau,q}$ in Eq. (6.3) at the crossover scale $q = q_{\rm th}$. This yields an estimate for the nonequilibrium prefactor

$$c_{\tau,\lambda} = \frac{\tilde{T}_{\tau,\lambda}}{uq_{\rm th}^2}. \tag{6.4}$$

The off-diagonal densities $m_{\tau,q}$ are decaying in the long-time limit, with $m_{\tau,q} \to 0$ in the limit $\tau \to \infty$. Their time evolution is shown in Fig. 3 for the same quench parameters as used for the diagonal densities. For momenta larger than the crossover scale $q_{\rm th}$, the off-diagonal densities decay exponentially fast in momentum, while they remain close to their initial value m_λ for momenta smaller than the crossover. The number of scattering events into the off-diagonal modes is proportional to $\Gamma^K_{\tau,q}$, which decreases in time very fast $\sim m^2_{\tau,q}$. This stands in contrast to the large number of out-scattering processes, which are given by $\sigma^R_{\tau,q} m_{\tau,q} \sim n_{\tau,q} m_{\tau,q}$ and dominate over the ingoing scattering events for a thermalizing diagonal distribution.

B. Fermion Green's function

The fermionic lesser Green's function $G^<_{t,x}$ can be computed using the time-evolved densities according to Eq. (2.17). The numerically determined fermion Green's function for a quench scenario with $\lambda = 1.6$ are shown in Fig. 4, as discussed in the beginning of the section. One can identify three spatiotemporal regimes, with individually different, generic scaling behavior described by Eqs. (3.3)–(3.6). By exploiting the generic form of the time-evolved phonon densities for interacting Luttinger

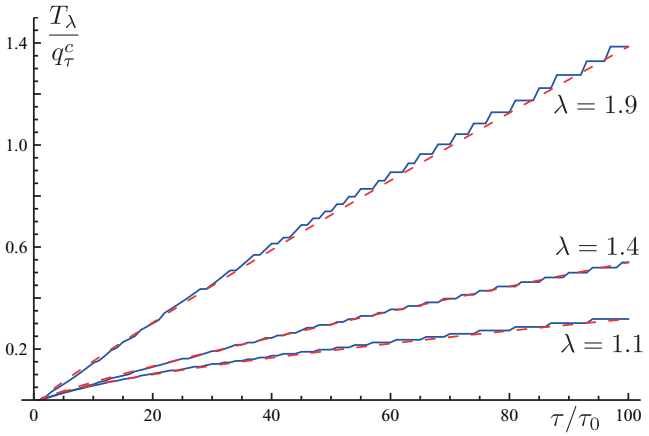

FIG. 4. Time evolution of the thermal length scale $T_\lambda x_{\rm th}(\tau) = \frac{T_\lambda}{q_{\rm th}(\tau)}$ for three different quench scenarios $\lambda = (1.1, 1.4, 1.9)$, normalized with the corresponding final temperature T_λ. The thermal length scale evolves according to a power law in time $T_\lambda x_{\rm th}(\tau) = x_\lambda \tau^{\alpha_\lambda}$, where both the amplitude and exponent depend nontrivially on the quench parameter and the exponent is invariant under a basis transformation from the dimensionless basis to the microscopic basis. In the present example, $\alpha_{1.1} = 0.7$, $\alpha_{1.4} = 0.85$, and $\alpha_{1.9} = 0.92$. The exponent is bounded from above $\alpha_\lambda < 1$ due to the subleading nature of the interactions and from below $0 < \alpha_\lambda$ by stability properties. For exponents $\alpha_\lambda < 1$, the thermalization dynamics will always feature a finite spatiotemporal prethermalized region as indicated in Fig. 1.

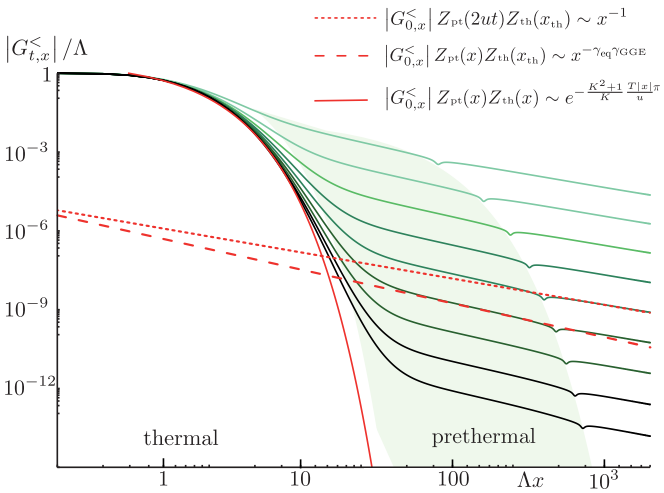

FIG. 5. Numerical results for the absolute value of the fermionic lesser Green's function $G^<_{t,x}$ (green solid lines) after a quench with $\lambda = 1.6$ for different times $t = \frac{40}{u\Lambda} l$, $l = 1, \ldots, 9$ (magnitude decreasing with l). The initial state corresponds to noninteracting fermions ($K = 1$) and the interaction was chosen such that $v_0\Lambda^2 = \frac{u\Lambda}{4}$. The figure illustrates the two crossovers and the three different spatiotemporal regimes of the Green's function. The red lines are determined according to the factorization (3.3)–(3.6) in the different regimes and describe the Green's function very well apart from the crossover regions.

liquids, we will in the following derive the form of the fermionic Green's function as given in Eq. (3.3).

In order to approximate the contribution from the off-diagonal densities, we exploit the fact that they remain close to their initial value $m_{\tau,q} \approx m_\lambda$ for momenta smaller than the crossover $q < q_{\rm th}$ and decay exponentially for larger momenta, yielding a negligible influence on short distances. To account for this behavior, we replace in the corresponding integrals the cutoff $\Lambda \to q_{\rm th}$ by the thermal crossover and approximate $m_{\tau,q} \approx m_\lambda$ for small momenta. The result is

$$\mathcal{G}^<_{t,x} = \mathcal{G}^<_{0,x} + i m_\lambda \ln\left(\frac{1+q_{\rm th}^2(x-2ut)^2}{1+q_{\rm th}^2(x+2ut)^2}\right) - i\frac{(K^2-1)m_\lambda}{2K} \times \ln\left[\frac{\left(1+q_{\rm th}^2(x+2ut)^2\right)\left(1+q_{\rm th}^2(x-2ut)^2\right)}{\left(1+4u^2t^2q_{\rm th}^2\right)^2\left(1+x^2q_{\rm th}^2\right)^2}\right] + i\frac{K^2+1}{K}\int_q \frac{2\pi e^{-|q|/\Lambda}}{|q|}(\cos(qx)-1)(n_{t,q}-n_\lambda). \tag{6.5}$$

In this expression, $\mathcal{G}_{0,x}$ contains again the initial postquench exponent; the terms proportional to m_λ represent the time-dependent contributions stemming from the off-diagonal densities, whereas the first term vanishes for distances away from the prethermal crossover $x \neq 2ut$ and the second term vanishes for distances $x < 1/q_{\rm th}(\tau) = x_{\rm th}(\tau)$ smaller than the thermal length. The latter expresses the fact that off-diagonal occupations vanish in the asymptotic thermal limit. The term in the third line of Eq. (6.5) takes into account the deviation of the diagonal phonon occupation from the flat initial distribution. Applying Eq. (6.3) to the third line of (6.5) with a smooth crossover function $\sim \exp(-|q|/q_{\rm th})$, $1 - \exp(-|q|/q_{\rm th})$, respectively, amounts to

$$\mathcal{G}^<_{t,x} = \mathcal{G}^<_{0,x} - i\frac{K^2-1}{2K} m_\lambda \ln \times\left[\frac{\left[1+q_{\rm th}^2(x+2ut)^2\right]\left[1+q_{\rm th}^2(x-2ut)^2\right]}{\left(1+4u^2t^2q_{\rm th}^2\right)^2\left(1+x^2q_{\rm th}^2\right)^2}\right] - 2\pi i\frac{K^2+1}{K}\frac{\tilde{T}_{\tau,\lambda}}{u}\left[\frac{q_{\rm th}^2x^2}{1+q_{\rm th}^2x^2} + |x|\left(1-\frac{2\arctan(q_{\rm th}|x|)}{\pi}\right)\right], \tag{6.6}$$

yielding the form of the fermionic Green's function in Eqs. (3.3)–(3.6). The prethermal amplitude $Z_{\rm pt}$ is determined by the contribution $\sim m_\lambda$ in the first line of Eq. (6.6), while the thermal amplitude $Z_{\rm th}$ is given by the exponential of the $\sim \tilde{T}_{\tau,\lambda}$ term in the second line of Eq. (6.6). This form of the fermionic Green's function holds away from the crossover lines $|x| = 2ut$ and $x = x_{\rm th}(t)$. As shown in Fig. 5, it is a very good approximation for the fermionic Green's function and illustrates perfectly the different thermalization regimes and their scaling behavior.

The form of Eq. (6.6) allows us to estimate the distance x_c, below which the kinetic theory is applicable and which we have given already in Eq. (3.2). One realizes immediately that the prethermalization described by the first line of (6.6) is absent for $K = 1$, i.e., for a quench to the noninteracting theory. This is due to the absence of a coupling of the single-particle sector to the many-body sector of the theory. A clear condition for the applicability of the kinetic theory can be obtained by

comparing the time-dependent variation of the two lines of Eq. (6.6) with each other. A well-defined prethermal plateau has then been established for |1st line of (6.6)| > |2nd line of (6.6)|, which leads to the condition on the distance $x < x_c(t)$, where $x_c(t)$ is given in Eq. (3.2).

We want to close the section by a discussion of the way in which the microscopic scales enter the thermalization dynamics discussed in the present context. For the noninteracting Luttinger liquid in equilibrium, the microscopic details are completely encoded in the sound velocity u and the Luttinger parameter K as well as the temperature of the system $T \geqslant 0$ and the Luttinger cutoff Λ. For a nonequilibrium setting in the quadratic Luttinger framework, one has to add the information on the initial state, which in the case of an interaction quench can be summarized in a single quench parameter λ. In the presence of interactions, we added the cubic vertex $\sim v_0$. This lead to the emergence of a crossover scale $x_{\rm th}(t)$, below which the system is effectively thermal, described by an effective time-dependent temperature $\tilde{T}_{t,\lambda}$. In the effective description of a factorizing Green's function, these quantities are sufficient to describe the postquench dynamics.

In the next section, we will discuss the time-dependent temperature and find $\tilde{T}_{\lambda,\tau} = T_\lambda + \Delta_\lambda \tau^{-\mu}$, where T_λ is the final temperature of the system, depending on the energy induced by the quench and Δ_λ the quench-dependent amplitude, while μ is a universal exponent. In original units, $\tilde{T}_{t,\lambda} = T_\lambda + u\Lambda\Delta_\lambda(v_0\Lambda^2 t)^{-\mu}$. In the simplified picture, these are the only relevant quantities, which show a functional dependence on the nonlinearity v_0, naturally containing the limit $v_0 \to 0$, for which the thermal crossover is at zero distance and the temperature is not defined due to the absence of thermalization.

The thermalization dynamics for interacting Luttinger liquids presented so far is not restricted to interaction quenches or global quenches in general but is expected to represent quite generically the relaxation dynamics of Luttinger liquids out of equilibrium. First of all, the dephasing of the off-diagonal modes due to the quadratic Hamiltonian will be present in any setup for which off-diagonal modes have been excited in the initial state and it spreads in space with the light cone $x = 2ut$. On the other hand, due to U(1) symmetry and the imposed scaling of the one-loop correction $\sim q$ for small momenta q [57], the change in the diagonal phonon distribution has to scale $\sim|q|$ as well. The determination of the crossover scale thus proceeds along the same lines as outlined above and thus separating thermalized short-distance modes with occupation $n_{t,q} \sim 1/|q|$ from nonthermal long-distance modes $n_{t,q} - n_{0,q} \sim |q|$, leading to a similar three-stage process for equilibration as described in the present setup.

C. Asymptotic thermalization in the resonant approximation

After the quench, momentum modes larger than the temporally decreasing crossover momentum $q_{\rm th}$ establish a local detailed balance between in- and out-scattering processes. This in turn defines the thermalized region in real space, for which, for distances $x < x_{\rm th}(t) = 1/q_{\rm th}(t)$, the fermionic Green's function has the typical thermal form. In this regime, the corresponding momentum modes for $q > q_{\rm th}$ are described by a single well-defined temperature $\tilde{T}_{t,\lambda}$ such that $n_{t,q} = n_{\rm B}(u|q|,T) \approx T/u|q|$. For momenta $q < q_{\rm th}$ the phonon distribution is however smaller than the corresponding thermal distribution $u|q|n_{t,q} < T$ (see Fig. 3) and in order to reach equipartition, energy has to be shifted from the thermal regime to the nonthermalized infrared modes. Consequently, the effective temperature of the high-momentum modes is decreasing in time, expressing the energy flow from the high- to the low-momentum regime, i.e., $\tilde{T}_{t\to\infty,\lambda} \to T_\lambda$ in the limit $x_{\rm th}(t) \to \infty$. The local equipartition of energy in the thermal regime is a consequence of a locally established detailed balance between in- and out-scattering processes. This local detailed balance in combination with exact energy conservation enforces that the energy transport to the long-wavelength modes in the system is performed by a global mechanism, which reveals the presence of dynamical slow modes in the system. They are a consequence of exact conservation laws, i.e., global symmetries, and in the present system emerge as a consequence of exact momentum and energy conservation. These modes are hydrodynamic gapless modes featuring an algebraic decay of the temperature in time towards its final value.

In order to determine the asymptotic dynamics in the thermalized regime, we define a momentum- and time-dependent temperature by inverting the on-shell Bose distribution function

$$\tilde{T}_{t,\lambda,q} = \frac{u|q|}{\ln\left(\frac{n_{t,q}+1}{n_{t,q}}\right)}. \tag{6.7}$$

The time evolution of $\tilde{T}_{t,\lambda,q}$ is shown in Fig. 6. For momenta $q < q_{\rm th}$ it varies as a function of momentum, indicating that the system has not thermalized on this scale and the notion of a temperature is absent. On the other hand, for momenta $q > q_{\rm th}$, $\tilde{T}_{t,\lambda,q}$ becomes momentum independent and a global property of the high-momentum modes. The decay of $\tilde{T}_{t,\lambda} = \tilde{T}_{t,q>q_{\rm th},\lambda}$ follows a power law in time, which can be expressed

$$\tilde{T}_{t,\lambda} = T_\lambda + u\Lambda\Delta_\lambda(v_0\Lambda^2 t)^{-\mu}, \tag{6.8}$$

where μ is the relaxation exponent associated with the dynamical slow modes. For a one-dimensional system with energy- and momentum-conserving dynamics $\mu = 2/3$, since this behavior corresponds to the Kardar-Parisi-Zhang universality class [74,78–81]. Performing a single parameter fit from the numerical simulations, we find that for long times $\mu = 2/3$ agrees very well with the numerical data for various different quench scenarios. However, for intermediate times, we find scaling behavior with $\mu > 2/3$ for some quenches, which might be traced back to the presence of subleading correction terms due to couplings to other diffusive modes [71,82,83]. Numerically a distinction of these possible scaling contributions is only possible for simulation times of multiple decades such that we cannot exclude a different exponent $\mu < 2/3$ at the longest times [71], which is however not observed in our simulations.

While the establishment of a local detailed balance, leading to effective thermalization and thermal-like fermionic correlation functions, is an effect of local quasiparticle scattering, the asymptotic thermalization dynamics describing energy transport over large distances in momentum space is determined by macroscopic diffusive modes in the system. This is observable by an algebraically decaying temperature towards

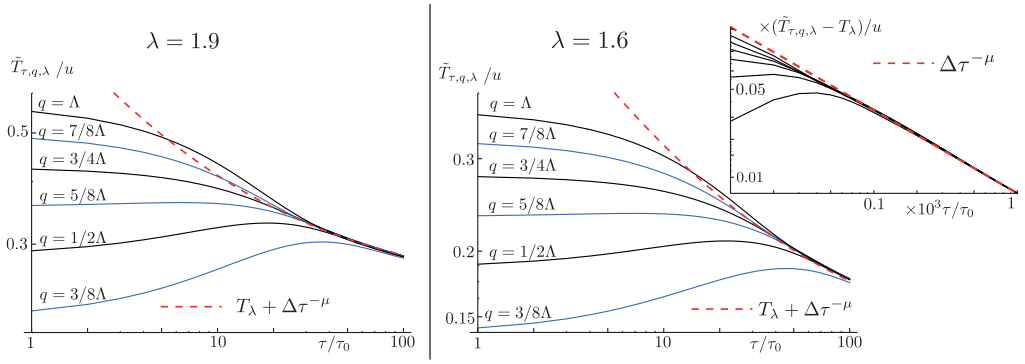

FIG. 6. Momentum-dependent temperature $\tilde{T}_{\tau,q,\lambda}$ as defined in Eq. (6.7) after two distinct quenches. For momenta smaller than the crossover $q_{\rm th}$, the temperature is a momentum-dependent function and cannot be seen as a global property. On the other hand, for momenta $q > q_{\rm th}$, the modes are described by the same temperature, indicating the presence of local detailed balance in the momentum regime larger than the crossover. In this regime, the temperature decays algebraically, revealing energy transport from the thermalized to the nonthermalized region, carried by dynamical slow modes. The inset shows the decay of the effective temperature for large times, allowing for the numerical estimate $\mu = 2/3$, which corresponds to the red dotted line.

the final temperature of the system T_λ. The discussion of the dynamical slow modes remains valid even in the presence of off-resonance scattering processes and therefore the universal properties of the asymptotic thermalization process remain unmodified. However, nonuniversal properties such as the final temperature and the relaxation rate will be modified by the off-resonance processes. Their precise computation would be a task for numerical simulations.

VII. CONCLUSION

In this work we have analyzed the relaxation dynamics of interacting Luttinger liquids, microscopically represented by one-dimensional interacting fermions with band curvature, after a sudden quench in the fermionic interaction. The theoretical analysis is based on quantum kinetic equations for the phonon distribution function and nonperturbative Dyson-Schwinger equations, which are both well suited to determine the time evolution of static observables for interacting Luttinger liquids with resonant cubic interactions and applicable in a broad parameter regime within the Luttinger framework. The central result is a two-step thermalization procedure including a spatiotemporal prethermalized regime for intermediate distances and times, which leads to fermionic correlation functions described by a generalized Gibbs state on these distances and corresponds to fast quasiparticle formation after the quench. For smaller distances, a thermalized regime occurs due to the scattering and associated redistribution of energy between the quasiparticle modes. This regime is described by thermal correlation functions with a characteristic thermal correlation length and a thermal quasiparticle distribution with an effective temperature that decays algebraically in time towards its asymptotic value.

This work shows in which way thermalization and prethermalization occur and spread in space for RG-irrelevant, and in this sense weak, integrability-breaking interactions. In this setup both thermalization and prethermalization occur locally in space. While the prethermalized region spreads ballistically in space, the thermalized region spreads subballistically due to the subleading, RG-irrelevant nature of the interactions. This allows for a well-defined prethermal regime in time and space, which would not be possible for a constant momentum-independent scattering vertex, for which thermalization would occur immediately on all different length scales. This underpins the statement that typical candidates for clearly observable prethermalized regimes within generic thermalization dynamics are quasiparticle theories with RG-irrelevant interactions.

ACKNOWLEDGMENTS

We acknowledge valuable discussions with Alessio Recati. This research was supported by the German Research Foundation through the Institutional Strategy of the University of Cologne within the German Excellence Initiative (ZUK 81) and the European Research Council under the European Unions Horizon 2020 research and innovation program (Grant No. 647434) as well as the Deutsche Akademie der Naturforscher Leopoldina under Grants No. LPDS 2013-07 and No. LPDR 2015-01.

APPENDIX A: KELDYSH ACTION

In this Appendix we derive the Keldysh action for the interacting Luttinger liquid after the quench. The partition function as the generating functional of all possible correlation functions has the form

$$Z(t) = \mathrm{tr}\big(e^{-iHt}\rho_0 e^{iHt}\big), \tag{A1}$$

where t is the time, ρ_0 is the initial state at $t = 0$, and H is the Hamiltonian (2.10), since we are interested in bosonic correlation functions. In order to express the partition function in terms of a path integral, one inserts bosonic coherent states at each infinitesimal time step and derives in a straightforward way the action on the $(\pm)$ contour

$$Z(t) = \int \mathcal{D}[\bar{a}_{+,X},\bar{a}_{-,X},a_{+,X},a_{-,X}]e^{iS^{(\pm)}}, \tag{A2}$$

where $\mathcal{D}[\cdots]$ is the common functional measure on the $(\pm)$ contour, $X=(x,t)$ the spatiotemporal coordinate, and

$$\mathcal{S}^{(\pm)}=\int_X\sum_{\alpha=\pm}\alpha(\bar{a}_{\alpha,X}i\partial_t a_{\alpha,X}-H[\bar{a}_{\alpha,X},a_{\alpha,X}])+\mathcal{F} \quad \text{(A3)}$$

is the action on the $(\pm)$ contour. In the action (A3), the Hamiltonian is expressed in terms of $(\pm)$ fields by replacing the operators in Eq. (2.10) by complex fields. The functional $\mathcal{F}$ carries the information on the initial state (i.e., is the initial density matrix ρ_0 expressed in terms of the bosonic fields) and, depending on the precise initial stay, in general contains higher-order vertices of arbitrary power [84,85]. After performing the Keldysh rotation to classical and quantum fields $\bar{a}_c=(\bar{a}_+ +\bar{a}_-)/\sqrt{2}$, $\bar{a}_q=(\bar{a}_+ -\bar{a}_-)/\sqrt{2}$ in the action, one obtains the Keldysh action

$$\mathcal{S}=\int_{t,p}(\bar{a}_{c,p,t},\bar{a}_{q,p,t})\begin{pmatrix}0 & i\partial_t-u|q|-i0^+\\ i\partial_t-u|q|+i0^+ & 0\end{pmatrix}\times\begin{pmatrix}a_{c,p,t}\\ a_{q,p,t}\end{pmatrix} \quad \text{(A4)}$$

$$+\int'_{t,p,k}v_0\sqrt{|pk(p+k)|}\,[2\bar{a}_{c,k+p,t}a_{c,p,t}a_{q,k,t}+\bar{a}_{q,k+p,t}(a_{c,k,t}a_{c,p,t}+a_{q,k,t}a_{q,p,t})+\text{H.c.}]+\mathcal{F}. \quad \text{(A5)}$$

In this representation, the functional $\mathcal{F}$ contains only quantum fields [84–86] and, since it contains the information on the initial state, is uniquely determined by the complete set of irreducible correlation functions at $t=0$. In the present case, we consider an initial state, which is a thermal state corresponding to the prequench Hamiltonian and therefore the initial correlations correspond to thermal correlations, which, according to the Dzyaloshinkii-Larkin theorem [84], are only of quadratic order. In the basis of the prequench fields, which we label as $\bar{b}_{\alpha,p,t},b_{\alpha,p,t},\alpha=c,q$, $\mathcal{F}_{t=0}$ is therefore nothing but the thermal Keldysh self-energy

$$\mathcal{F}_{t=0}=2i0^+\int_p\bar{b}_{q,p,t=0}[2n(u|p|)+1]b_{q,p,t=0}, \quad \text{(A6)}$$

where $n(u|p|)$ is the Bose distribution. The transformation from the prequench to the postquench basis can be performed by subsequently applying the canonical Bogoliubov transformation (2.5) and (2.6) and reads

$$\bar{a}_{\alpha,p,t}=\frac{1}{2}\left[\sqrt{\lambda}(\bar{b}_{\alpha,p,t}-b_{\alpha,-p,t})+\frac{1}{\sqrt{\lambda}}(\bar{b}_{\alpha,p,t}+b_{\alpha,-p,t})\right]. \quad \text{(A7)}$$

Combining these results, the quantum part of the action can be expressed solely by the Keldysh self-energy

$$\mathcal{F}=\int_{p,t,t'}(\bar{a}_{q,p,t},a_{q,-p,t})\Sigma^K_{p,t,t'}\begin{pmatrix}a_{q,p,t'}\\ \bar{a}_{q,-p,t'}\end{pmatrix}, \quad \text{(A8)}$$

with the initial condition

$$\Sigma^K_{p,0,0}=\frac{2i0^+}{2\lambda}[2n(u|p|)+1]\begin{pmatrix}1+\lambda^2 & \lambda^2-1\\ \lambda^2-1 & \lambda^2+1\end{pmatrix}. \quad \text{(A9)}$$

The time evolution of the Keldysh self-energy and the corresponding phonon distribution function is determined via the kinetic equation approach in the main text.

APPENDIX B: FERMIONIC GREEN'S FUNCTIONS

In this Appendix we derive the expression for the exponent (2.13) in the fermionic Green's function (2.16). The fermionic lesser and greater Green's functions for right movers at equal times are defined as

$$G^<_{t,x}=-i\langle\bar{\psi}_{t,x}\psi_{t,0}\rangle=-i\langle\bar{\psi}_{-,t,x}\psi_{+,t,0}\rangle, \quad \text{(B1)}$$

$$G^>_{t,x}=-i\langle\psi_{t,x}\bar{\psi}_{t,0}\rangle=i\langle\bar{\psi}_{+,t,-x}\psi_{-,t,0}\rangle, \quad \text{(B2)}$$

where the second equality in both equations indicates the average with respect to the functional integral and the indices $\pm$ denote the corresponding contour. The corresponding Green's functions for left movers are obtained by $x\to -x$, as discussed in the main text. Obviously, in a spatially translationally invariant system, the greater Green's function is obtained from the lesser Green's function by a contour exchange $(+\leftrightarrow -)$ and spatial inversion $(x\to -x)$. Right-moving fermion operators are expressed in terms of Luttinger fields according to

$$\bar{\psi}_{\alpha,t,x}=\sqrt{\frac{\Lambda}{2\pi}}\,e^{ik_F x}e^{i(\phi_{\alpha,t,x}-\theta_{\alpha,t,x})}, \quad \text{(B3)}$$

where $\alpha=\pm$ labels the contour. It is important to perform the transformation (B3) on the $\pm$ and not on the Keldysh contour since the transformation to the Luttinger basis does not commute with the Keldysh rotation. The lesser Green's function expressed in terms of the Luttinger fields is

$$G^<_{t,x}=-i\frac{\Lambda}{2\pi}e^{ik_F x}\langle e^{i(\phi_{-,t,x}-\theta_{-,t,x}-\phi_{+,t,0}+\theta_{+,t,0})}\rangle=-i\frac{\Lambda}{2\pi}e^{ik_F x}e^{-(i/2)\mathcal{G}^<_{t,x}}. \quad \text{(B4)}$$

The exponent

$$\mathcal{G}^<_{t,x}=2i\ln\langle e^{i(\phi_{-,t,x}-\theta_{-,t,x}-\phi_{+,t,0}+\theta_{+,t,0})}\rangle \quad \text{(B5)}$$

is, according to the linked cluster theorem, nothing but the sum of all one-particle irreducible contractions of an expansion of the exponential. The generating functional for the one-particle irreducible contractions is the effective action $\Gamma[\bar{a}_{\alpha,X},a_{\alpha,X}]$, which we determine up to cubic order by Dyson-Schwinger equations. The four-point irreducible vertex is subleading and negligibly small on all relevant scales. On the other hand, the three-body irreducible vertex remains local [57] and therefore in the expansion of the exponential (B4), only purely local terms (e.g., $\sim\theta^3_{t,x}$) give a contribution at cubic order. Due to translational invariance, these contributions yield only a constant amplitude for the Green's function, which, due to the Green's function, must be unity. Consequently, only the quadratic terms contribute to the expansion and the sum of all quadratic irreducible vertices is the full Green's function, i.e.,

$$\mathcal{G}^<_{t,x}=-i\langle(\phi_{-,t,x}-\theta_{-,t,x}-\phi_{+,t,0}+\theta_{+,t,0})^2\rangle. \quad \text{(B6)}$$

Performing the Keldysh rotation, one straightforwardly arrives at the expression for the exponent (2.16).

The various Green's functions can be evaluated using the Bogoliubov transformation to the phonon basis, which yields the set of Green's functions

$$G^R_{\theta\theta,t,x}=G^R_{\phi\phi,x,t}=0, \quad \text{(B7)}$$

$$G^K_{\phi\phi,t,x} = \int_q \frac{\pi K}{|q|}\left[G^K_{t,q} + i\,\mathrm{Im}\left(G^{KA}_{t,q}\right)\right]\cos(qx)e^{-|q|/\Lambda}, \quad \text{(B8)}$$

$$G^K_{\theta\theta,t,x} = \int_q \frac{\pi}{|q|K}\left[G^K_{t,q} - i\,\mathrm{Im}\left(G^{KA}_{t,q}\right)\right]\cos(qx)e^{-|q|/\Lambda}, \quad \text{(B9)}$$

$$\begin{aligned} G^R_{\theta\phi,t,x} - G^A_{\theta\phi,t,x} &= -i\int_q \frac{\pi}{q}\sin(qx)\left(G^R_{t,q} - G^A_{t,q}\right)e^{-|q|/\Lambda} \\ &= -\arctan(\Lambda x), \end{aligned} \quad \text{(B10)}$$

$$G^K_{\theta\phi,t,x} = -i\int_q \frac{\pi}{q}\sin(qx)\mathrm{Re}\left(G^{KA}_{t,q}\right)e^{-|q|/\Lambda}. \quad \text{(B11)}$$

Here $G^K_{t,q} = -i\langle a_{c,q,t}\bar{a}_{c,q,t}\rangle = -i(2n_{t,q}+1)$ is the equal-time diagonal Keldysh Green's function and $G^{KA}_{t,q} = -i\langle \bar{a}_{c,-q,t}\bar{a}_{c,q,t}\rangle = -i2m_{t,q}e^{2iu|q|t}$ is the anomalous equal-time Keldysh Green's function. Inserting these expressions in the exponent (2.16), one finds (2.17), which is $\mathcal{G}^<_{t,x}$ for equal times up to fourth-order irreducible vertex corrections.

[1] A. Polkovnikov, K. Sengupta, A. Silva, and M. Vengalattore, Rev. Mod. Phys. **83**, 863 (2011).
[2] M. Rigol, A. Muramatsu, and M. Olshanii, Phys. Rev. A **74**, 053616 (2006).
[3] M. Rigol, V. Dunjko, V. Yurovsky, and M. Olshanii, Phys. Rev. Lett. **98**, 050405 (2007).
[4] M. Kollar, F. A. Wolf, and M. Eckstein, Phys. Rev. B **84**, 054304 (2011).
[5] M. Rigol, V. Dunjko, and M. Olshanii, Nature (London) **452**, 854 (2008).
[6] M. A. Cazalilla, Phys. Rev. Lett. **97**, 156403 (2006).
[7] P. Calabrese and J. Cardy, Phys. Rev. Lett. **96**, 136801 (2006).
[8] T. Barthel and U. Schollwöck, Phys. Rev. Lett. **100**, 100601 (2008).
[9] F. D. M. Haldane, Phys. Rev. Lett. **47**, 1840 (1981).
[10] F. D. M. Haldane, J. Phys. C: Solid State Phys. **14**, 2585 (1981).
[11] T. Giamarchi, *Quantum Physics in One Dimension*, International Series of Monographs on Physics (Oxford University Press, Oxford, 2004).
[12] A. Iucci and M. A. Cazalilla, Phys. Rev. A **80**, 063619 (2009).
[13] A. Iucci and M. A. Cazalilla, New J. Phys. **12**, 055019 (2010).
[14] M. Greiner, O. Mandel, T. W. Hänsch, and I. Bloch, Nature (London) **419**, 51 (2002).
[15] T. Kinoshita, T. Wenger, and D. S. Weiss, Nature (London) **440**, 900 (2006).
[16] S. Hofferberth, I. Lesanovsky, B. Fischer, T. Schumm, and J. Schmiedmayer, Nature (London) **449**, 324 (2007).
[17] W. Rohringer, D. Fischer, F. Steiner, I. E. Mazets, J. Schmiedmayer, and M. Trupke, Sci. Rep. **5**, 9820 (2015).
[18] M. Gring, M. Kuhnert, T. Langen, T. Kitagawa, B. Rauer, M. Schreitl, I. Mazets, D. A. Smith, E. Demler, and J. Schmiedmayer, Science **337**, 1318 (2012).
[19] F. Meinert, M. J. Mark, E. Kirilov, K. Lauber, P. Weinmann, A. J. Daley, and H.-C. Nägerl, Phys. Rev. Lett. **111**, 053003 (2013).
[20] F. Meinert, M. J. Mark, E. Kirilov, K. Lauber, P. Weinmann, M. Gröbner, A. J. Daley, and H.-C. Nägerl, Science **344**, 1259 (2014).
[21] P. M. Preiss, R. Ma, M. E. Tai, A. Lukin, M. Rispoli, P. Zupancic, Y. Lahini, R. Islam, and M. Greiner, Science **347**, 1229 (2015).
[22] S. Hild, T. Fukuhara, P. Schauß, J. Zeiher, M. Knap, E. Demler, I. Bloch, and C. Gross, Phys. Rev. Lett. **113**, 147205 (2014).
[23] M. Cheneau, P. Barmettler, D. Poletti, M. Endres, P. Schauß, T. Fukuhara, C. Gross, I. Bloch, C. Kollath, and S. Kuhr, Nature (London) **481**, 484 (2012).
[24] T. Langen, S. Erne, R. Geiger, B. Rauer, T. Schweigler, M. Kuhnert, W. Rohringer, I. E. Mazets, T. Gasenzer, and J. Schmiedmayer, Science **348**, 207 (2015).
[25] K. Agarwal, E. G. D. Torre, B. Rauer, T. Langen, J. Schmiedmayer, and E. Demler, Phys. Rev. Lett. **113**, 190401 (2014).
[26] T. Langen, R. Geiger, M. Kuhnert, B. Rauer, and J. Schmiedmayer, Nat. Phys. **9**, 640 (2013).
[27] M. Moeckel and S. Kehrein, Phys. Rev. Lett. **100**, 175702 (2008).
[28] M. Stark and M. Kollar, arXiv:1308.1610.
[29] J. Berges, S. Borsányi, and C. Wetterich, Phys. Rev. Lett. **93**, 142002 (2004).
[30] M. Eckstein, M. Kollar, and P. Werner, Phys. Rev. Lett. **103**, 056403 (2009).
[31] F. H. L. Essler, S. Kehrein, S. R. Manmana, and N. J. Robinson, Phys. Rev. B **89**, 165104 (2014).
[32] A. Rosch, D. Rasch, B. Binz, and M. Vojta, Phys. Rev. Lett. **101**, 265301 (2008).
[33] M. Marcuzzi, J. Marino, A. Gambassi, and A. Silva, Phys. Rev. Lett. **111**, 197203 (2013).
[34] N. Nessi and A. Iucci, arXiv:1503.02507.
[35] M. Fagotti, J. Stat. Mech. (2014) P03016.
[36] B. Bertini and M. Fagotti, J. Stat. Mech. (2015) P07012.
[37] M. Babadi, E. Demler, and M. Knap, Phys. Rev. X **5**, 041005 (2015).
[38] B. Bertini, F. H. L. Essler, S. Groha, and N. J. Robinson, Phys. Rev. Lett. **115**, 180601 (2015).
[39] M. Srednicki, Phys. Rev. E **50**, 888 (1994).
[40] J. M. Deutsch, Phys. Rev. A **43**, 2046 (1991).
[41] J. W. Gibbs, Trans. Conn. Acad. Arts Sci. **3**, 108 (1874–1878).
[42] G. Biroli, C. Kollath, and A. M. Läuchli, Phys. Rev. Lett. **105**, 250401 (2010).
[43] P. Debray, V. Zverev, O. Raichev, R. Klesse, P. Vasilopoulos, and R. S. Newrock, J. Phys.: Condens. Matter **13**, 3389 (2001).
[44] P. Debray, V. N. Zverev, V. Gurevich, R. Klesse, and R. S. Newrock, Semicond. Sci. Technol. **17**, R21 (2002).
[45] A. F. Andreev, Sov. Phys. JETP **51**, 1038 (1980).
[46] K. V. Samokhin, J. Phys.: Condens. Matter **10**, L533 (1998).
[47] M. Punk and W. Zwerger, New J. Phys. **8**, 168 (2006).
[48] M. Pustilnik, E. G. Mishchenko, L. I. Glazman, and A. V. Andreev, Phys. Rev. Lett. **91**, 126805 (2003).
[49] M. Khodas, M. Pustilnik, A. Kamenev, and L. I. Glazman, Phys. Rev. B **76**, 155402 (2007).
[50] A. Imambekov and L. I. Glazman, Science **323**, 228 (2009).
[51] A. Imambekov and L. I. Glazman, Phys. Rev. Lett. **102**, 126405 (2009).
[52] T. Price and A. Lamacraft, Phys. Rev. B **90**, 241415 (2014).
[53] T. Price and A. Lamacraft, arXiv:1509.08332.
[54] A. Kamenev, *Field Theory of Non-Equilibrium Systems* (Cambridge University Press, Cambridge, 2011).

[55] M. Tavora, A. Rosch, and A. Mitra, Phys. Rev. Lett. **113**, 010601 (2014).
[56] M. Tavora and A. Mitra, Phys. Rev. B **88**, 115144 (2013).
[57] M. Buchhold and S. Diehl, Eur. Phys. J. D **69**, 224 (2015).
[58] A. Rozhkov, Eur. Phys. J. B **47**, 193 (2005).
[59] I. V. Protopopov, D. B. Gutman, and A. D. Mirlin, Phys. Rev. B **90**, 125113 (2014).
[60] A. Imambekov and L. I. Glazman, Phys. Rev. Lett. **100**, 206805 (2008).
[61] R. G. Pereira, J. Sirker, J.-S. Caux, R. Hagemans, J. M. Maillet, S. R. White, and I. Affleck, Phys. Rev. Lett. **96**, 257202 (2006).
[62] M. Pustilnik, M. Khodas, A. Kamenev, and L. I. Glazman, Phys. Rev. Lett. **96**, 196405 (2006).
[63] M. Heyl, S. Kehrein, F. Marquardt, and C. Neuenhahn, Phys. Rev. B **82**, 033409 (2010).
[64] A. Imambekov, T. L. Schmidt, and L. I. Glazman, Rev. Mod. Phys. **84**, 1253 (2012).
[65] D. N. Aristov, Phys. Rev. B **76**, 085327 (2007).
[66] M. Heyl and M. Vojta, Phys. Rev. B **92**, 104401 (2015).
[67] D. Forster, D. R. Nelson, and M. J. Stephen, Phys. Rev. A **16**, 732 (1977).
[68] D. A. Smith, M. Gring, T. Langen, M. Kuhnert, B. Rauer, R. Geiger, T. Kitagawa, I. Mazets, E. Demler, and J. Schmiedmayer, New J. Phys. **15**, 075011 (2013).
[69] S. Trotzky, Y.-A. Chen, A. Flesch, I. P. McCulloch, U. Schollwock, J. Eisert, and I. Bloch, Nat. Phys. **8**, 325 (2013).
[70] X.-W. Guan, M. T. Batchelor, and C. Lee, Rev. Mod. Phys. **85**, 1633 (2013).
[71] J. Lux, J. Müller, A. Mitra, and A. Rosch, Phys. Rev. A **89**, 053608 (2014).
[72] C. Karrasch, J. Rentrop, D. Schuricht, and V. Meden, Phys. Rev. Lett. **109**, 126406 (2012).
[73] D. M. Kennes and V. Meden, Phys. Rev. B **88**, 165131 (2013).
[74] M. Kulkarni and A. Lamacraft, Phys. Rev. A **88**, 021603 (2013).
[75] M. Arzamasovs, F. Bovo, and D. M. Gangardt, Phys. Rev. Lett. **112**, 170602 (2014).
[76] M. Buchhold and S. Diehl, Phys. Rev. A **92**, 013603 (2015).
[77] G. D. Mahan, *Many-Particle Physics*, 2nd ed. (Plenum, New York, 1990).
[78] M. Kardar, G. Parisi, and Y. C. Zhang, Phys. Rev. Lett. **56**, 889 (1986).
[79] M. Prähofer and H. Spohn, J. Stat. Phys. **115**, 255 (2004).
[80] H. van Beijeren, Phys. Rev. Lett. **108**, 180601 (2012).
[81] J. Quastel and H. Spohn, J. Stat. Phys. **160**, 965 (2015).
[82] O. Narayan and S. Ramaswamy, Phys. Rev. Lett. **89**, 200601 (2002).
[83] S. Mukerjee, V. Oganesyan, and D. Huse, Phys. Rev. B **73**, 035113 (2006).
[84] D. B. Gutman, Y. Gefen, and A. D. Mirlin, Europhys. Lett. **90**, 37003 (2010).
[85] D. B. Gutman, Y. Gefen, and A. D. Mirlin, Phys. Rev. B **81**, 085436 (2010).
[86] I. Chernii, I. P. Levkivskyi, and E. V. Sukhorukov, Phys. Rev. B **90**, 245123 (2014).